Concentrated, "pulsed" axial glacier flow: structural glaciological evidence from Kvíárjökull in SE Iceland

Authors

Emrys Phillips [1]*, Jez Everest [1], David J.A. Evans [2], Andrew Finlayson [1], Marek Ewertowski [2, 3], Ailsa Guild [1, 2] and Lee Jones [4]

Author affiliations

1. British Geological Survey, The Lyell Centre, Research Avenue South, Edinburgh EH14 4AP

2. Department of Geography, Durham University, South Road, Durham DH1 3LE

3. Adam Mickiewicz University, Dziegielowa 27, 61-680 Poznan, Poland

4. British Geological Survey, Keyworth, Nottingham NG12 5GG, UK

** Corresponding author*

Telephone: +44 (0)131-667-0342; Email - erp@bgs.ac.uk

Abstract

A detailed structural glaciological study carried out on Kvíárjökull in SE Iceland reveals that recent flow within this maritime glacier is concentrated within a narrow corridor located along its central axis. This active corridor is responsible for feeding ice from the accumulation zone on the south-eastern side of Öræfajökull to the lower reaches of the glacier and resulted in a c. 200 m advance during the winter of 2013-14 and the formation of a push-moraine. The corridor comprises a series of lobes linked by a laterally continuous zone of highly fractured ice characterised by prominent flow-parallel crevasses, separated by shear zones. The lobes form highly crevassed topographic highs on the glacier surface and occur immediately down-ice of marked constrictions caused by prominent bedrock outcrops located on the northern side of the glacier. Close to the frontal margin of Kvíárjökull, the southern side of the glacier is relatively smooth and pock-marked by a number of large moulins. The boundary between this slow moving ice and the active corridor is marked by a number of ice flow-parallel strike-slip faults and a prominent dextral shear zone which resulted in the clockwise rotation and dissection of an ice-cored esker exposed on the glacier surface. It is suggested that this

concentrated style of glacier flow identified within Kvíárjökull has affinities with the individual flow units which operate within pulsing or surging glaciers.

Key Words

Structural glaciology, concentrated axial glacier flow, pulse surge-like behaviour, Kvíárjökull, SE Iceland

Introduction

Published structural glaciological studies have largely focused upon those structures associated with glacier advance from a wide range of dynamic settings, including polythermal (Hambrey *et al*., 2005), surging (Sharp, 1988; Sharp *et al*., 1988; Lawson *et al*., 1994; Lawson, 1996; Bennett *et al*., 2000; Woodward *et al*., 2002), Arctic (Huddleston and Hooke, 1980) and alpine glaciers (Allen et al., 1960; Hambrey and Milnes, 1977; Glasser *et al*., 2003; Goodsell *et al*., 2005; Herbst *et al*., 2006; Appleby *et al*., 2010). Furthermore a small number of recent studies have investigated the deformation occurring within the ice during stagnation and collapse (e.g. Glasser and Scambos, 2008; Phillips *et al*., 2013). These studies have not only contributed to our understanding of the strain histories and structural evolution of glaciers and ice sheets, but have also shed light on the mechanisms controlling their forward movement. The traditional view of the movement of a non-surging valley glacier is that it largely acts as a single "plug flow" where the entire glacier body moves "en-masse" down valley, even though it comprises numerous individual flow units fed by discrete feeder basins in its upper accumulation zone. As a result the crevasse patterns observed on the surface of valley glaciers are typically interpreted in terms of the lateral shear stresses imposed at the glacier margin (Sharp *et al*., 1988; Benn and Evans, 2010; Colgan *et al*., 2016), or as a combination of lateral shear and longitudinal compressive stresses imposed by the forward motion of the ice (Sharp *et al*., 1988; Benn and Evans, 2010). Compressional flow increases towards the leading edge of the "plug flow" and is therefore thought to be largely responsible for the observed increase in thrusting near to the snouts of many glaciers (Hambrey and Huddart, 1995; Hambrey and Dowdeswell, 1997; Glasser *et al*., 1998; Hambrey *et al*., 1999; Murray *et al*., 2000). Flow within large ice streams as they drain both contemporary and former ice sheets is clearly partitioned into a series of flow zones (Joughin *et al*., 2002; Bennett, 2003 and references therein; Truffer and Echelmeyer, 2003; Hulbe and Fahnestock, 2004, 2007). The "footprint" of these flow zones may be preserved in the geomorphological records of palaeo ice streams, specifically within juxtaposed corridors of flow-sets defined by elongate subglacial landforms (drumlins, megascale lineations, flutings), ribbed terrain, shear margin moraines and crevasse-squeeze ridges (e.g. Dyke and Morris, 1988; Dyke *et al*., 1992; Stokes and Clark, 2002; Kleman and Glasser, 2007; Stokes *et al*., 2007, 2008; O' Cofaigh *et al*., 2010; Evans *et al*., 2016). The presence of discrete flow zones within valley glaciers is also well known and has been previously associated with debris transfer pathways in particular (e.g. Eyles and Rogerson, 1978; Hambrey and Lawson, 2000; Hambrey and Glasser, 2003; Jennings *et al*., 2014), but our understanding of their role in glacier dynamics and glacial geomorphology remains to be fully elucidated for a wider range of glacierization styles, especially in light of increasing rates of ice recession and variable dynamic responses to recent climate warming.

Recent advances in the quality and resolution of remotely sensed data (e.g. aerial photography, LiDAR, satellite imagery) means that the structural architecture of glaciers can be analysed in far greater detail, potentially shedding light on how ice is transferred from the accumulation zone, through the glacier to its snout. This paper presents the results of a detailed study of Kvíárjökull in southeast Iceland (Figure 1) combining a structural glaciological study with ground penetrating radar (GPR) and aerial photogrammetry surveys to investigate its surface (2D) and subsurface (3D) structure. The results enable the glacier to be divided into a number of structural domains based upon the variation in the orientation and style of brittle faulting and fracturing. This approach demonstrates that, rather than advancing as a single, predominantly integrated or "plug flow" unit, the most dynamic ice flow within this maritime glacier since the 1940s has been concentrated within a narrow corridor located along its central axis. Marked changes in the structure of the lower reaches of Kvíárjökull indicate that the volume of ice being fed through this corridor has changed over time. A conceptual model for the structural evolution of Kvíárjökull and its links to pulsed glacier flow from the 1940s to present is formulated. It is suggested that this concentrated style of glacier flow has affinities with the individual flow units which operate within pulsing or surging glaciers (e.g. Kamb *et al*. 1985; Kamb and Engelhardt 1987), the geomorphic impact of which have recently been identified for palaeo-ice streams by Colgan *et al*. (2003), Jennings (2006) and Evans *et al*. (2016).

Methodology

Understanding the structural evolution of Kvíárjökull between 1945 and 2014 required a multidisciplinary approach using the following methods.

Structural mapping

The structural mapping and analysis of the large-scale pattern of deformation structures exposed on the surface of Kvíárjökull was carried out using historical vertical aerial photographs, supplemented by field survey and more detailed field-based UAV (Unmanned Aerial Vehicle) aerial photography (see below). Digital scans of the five vertical analogue aerial photographs (National Land Survey of Iceland (LMI)) of the lower reaches of Kvíárjökull taken between 1945 and 2003 were orthorectified in LPS (Leica Photogrammetry Suite) and imported into ArcGIS 10.1. The high-resolution 2014 imagery used for structural mapping for the entire glacier (Figure 2) was captured by the WorldView-2 satellite of Digital Globe on September 23 at 13:02. A bundle product was used, comprising a panchromatic band (0.5 m ground sampling distance (GSD)) and 4 multispectral bands (2.0 m GSD). The image has been orthorectified using a DEM (Digital Elevation Model) and pansharpened to generate a 4-band multispectral image with 0.5 m GSD.

The various sets of faults and fractures, as well as the foliation banding (ogives) on the surface of Kvíárjökull were digitised using ArcGIS at a scale of between 1:500 and 1:1,000 depending upon the resolution of the photographs. Marked changes in the orientation of the main fracture sets were used to define a series (27 in total) of colour coded, structural domains (Figures 2 to 5). The orientation (strike) of the individual fractures was calculated using a Python Script macro (Diaz Doce 2014, unpublished) and the resultant dataset exported from ArcGIS and plotted on a series of rose diagrams using StereoStat by RockWorks ™ (see Figure 2). Detailed mapping of the structures observed within the marginal zone of the glacier (Figure 6) was achieved using the same methodology (digitisation at 1:300 scale) and the UAV-based aerial photography. High-resolution versions of the detailed maps shown in Figures 2 and 10 are provided as supplementary publications.

Field work carried out in August-September 2014 involved the recording of the orientation (dip, strike, dip azimuth), sense and amount of offset (where applicable), and inter-relationships between the various sets of faults, fractures and foliations (e.g. foliation banding). The orientations of the planar structures were measured using a compass clinometer (corrected for magnetic deviation -11.5°) with the data displayed on a series of lower hemisphere stereographic projections and rose diagrams. Due to the highly crevassed to "ridged" nature of the surface of Kvíárjökull (see Figures 1b and c) field studies were restricted to the area close to southeast-side of the glacier (corresponding to Domain 1 on Figure 3).

Ground Penetrating Radar survey

Ground Penetrating Radar (GPR) surveys were used to investigate ice thickness and structure in the southeastern frontal area of the glacier (Figure 7). A PulseEKKO Pro system with 100 MHz antennae was towed manually across 6.2 km of the glacier surface, using an odometer wheel to trigger data collection at 0.25 m intervals. Each trace was staked 8 times to increase signal-to-noise ratio. Survey lines were directed both parallel and perpendicular to glacier flow; however, a regular grid of lines could not be obtained due to the presence of large moulins, fractures and crevasses. Positional data were stored alongside every 5th GPR trace, and captured using a standalone Novatel SMART-V1 GPS antenna. GPR data from the glacier were processed using a dewow filter, 2D migration, SEC (spreading and exponential compensation) gain, and topographic correction. A radar wave velocity of 0.16 m ns^{-1} was used, based on the results of a common midpoint survey. An interpolation for the glacier bed (Figure 7b) was generated from bed elevation picks by performing a discrete smooth interpolation (Mallet, 2002) in the GoCad software program.

GPR profiles were also recorded on the foreland beyond the northeastern margin of the glacier to investigate subsurface evidence for repeated glacier push in that zone (Figure 7). Data were collected using 100 MHz antennae, in a similar fashion to the glacier surveys. Processing of the foreland radar surveys consisted of applying a dewow filter, average background subtraction, 2-D migration, and SEC gain. No common midpoint survey was conducted in the foreland. However, sections in the area revealed underlying damp sand. Therefore a radar wave velocity of 0.06 m ns^{-1} has been assumed (Sensors and Software, 2003; Cassidy *et al*., 2003; Kjær *et al*., 2004; Burke *et al*., 2008; Benediktsson *et al*., 2009; Benediktsson *et al*., 2010).

Digital aerial photogrammetry survey and time-lapse animation

UAV surveys were carried out in August/September 2014. Flights were performed by quadcopter equipped with a 14-megapixel camera mounted on a 3D gimbal system. The workflow proposed by Evans *et al*. (2015) was applied for processing of the acquired images in Agisoft Photoscan software. Images were georeferenced to the ISN93/Lambert 1993 projection using ground Topcon Hiper II dGPS system. Processing resulted in production of an orthomosaic with a 0.03 m GDS and DEM with 0.07 m GSD, which covers about 1.5 km^2 of the snout area enabling high-resolution structural mapping.

The time-laps animation (see supplementary publication) used to investigate the pattern of flow within Kvíárjökull was created using Landsat images for the 1985-2016 time period. Landsat scenes 217-015 (path-row) and 216-015 cover Kvíárjökull completely; however many scenes were unusable due to clouds or extensive snow coverage. Finally, 45 orthorectified scenes from Landsat 5 (Thematic Mapper sensor - TM), 7 (Enhanced Thematic Mapper Plus sensor (ETM+)) and 8 (Operational Land Imager sensor (OLI)) available at USGS server (http://earthexplorer.usgs.gov/) were selected. Instead of using LandsatLook products (which are provided as 30 m cell size and characterised by some artefacts related to the image compression), full multispectral scenes have been downloaded and processed. Composite images of mid-infrared – near-infrared – red bands (Bands 5, 4, and 3 for TM and ETM+; bands 6, 5, and 4 OLI) have been produced with 30 m pixel size for TM sensor and pansharpened to 15 m pixel size for ETM+ and OLI sensors. The colour composition used in this study shows glaciers in blue to cyan. Time-intervals between images are not even: in some cases, more than one image was available for specific year (e.g. 4 scenes for the year 1988, 1989 and 2013), whereas data for some periods were missing (1992-1993; 1995-1997, 2004-2005, 2007, 2012). Map compositions containing processed image and a frame with coordinates in UTM 28N projection were designed in ArcMap and exported to graphic file format. Animated time-series of images was provided as mp4 format and as an mp4 file (see supplementary publication).

Terrestrial LiDAR and Digital Elevation Model analysis

A terrestrial LiDAR survey was conducted based around the northern margin of Kvíárjökull, seeking to capture both glacier structure and architecture, and the proglacial geomorphology adjacent to this flank. This data was used to create a high resolution, georectified DEM of the glacier snout to form the basis of a surface change model to investigate the change in surface height over time. Data sets were captured using a Riegl VZ-1000 system at 8 mm scanning resolution, and accurately referenced to a common coordinate system. A high-resolution digital camera mounted on the scanner allowed for the capture of coloured point clouds (ASCII format data comprising x, y, z, intensity, and red-green-blue colour values). These data were orientated using the relative differential Global Navigation Satellite Systems (GNSS) positions of both the scanner and the back sights (in WGS84 27N) and, once processed, a Virtual Outcrop Model of the glacier and glacial margin were produced. The RiScanPro package was used to align individual scans and check for errors in orientation. Surface 3D DEMs were created using I-Site Studio.

Both aerial and terrestrially captured DEM datasets were normalised to a 2 m point spacing and combined into a unified surface using I-Site Studio (Figure 8), which was then overlaid onto a DTM surface produced by Veðurstofa Islands (the “Icelandic Meteorological Office”, IMO) in 2010 (Jóhannesson *et al*., 2013). This surface has an average measurement density of approximately one measurement every 3 m^2. The IMO measurements were averaged and interpolated onto a regular 5 x 5 m grid. Despite the inevitable lower resolution of the IMO DTM than that produced by this current study, the two surfaces are similar, allowing an elevation change model to be produced. This highlights raising and lowering of the 2014 glacier surface relative to the surface in 2010.

Location of study area and glaciological setting

Kvíárjökull is located ~250 km east of Reykjavık in southeast Iceland and is one of a number of temperate outlet glaciers which drain the south flank of the Öræfajökull ice-capped stratovolcano, the southernmost accumulation centre within the much larger Vatnajökull ice cap (Figure 1a). Like other Icelandic glaciers, Kvíárjökull is highly sensitive to climatic fluctuations on an annual to decadal scale and has over the last two decades been downwasting at an accelerated rate (Jóhannesson and Sigurðsson, 1998; Sigurðsson *et al*., 2007; Einarsson and Sigurðsson, 2015). The glacier, which is over 12 km long, descends via a steep icefall from its source area at over 1500 m above sea level (a.s.l.) (Figure 1b). The lower part of the glacier is confined within a deep valley formed to the north by the rugged highlands of Vatnafjöll, and to the south by Staðarfall (Figure 1b). At its margin the glacier forms a low-gradient piedmont lobe which occupies an overdeepened subglacial basin surrounded by a large Holocene latero-frontal moraine ridge (Evans *et al*., 1999; Spedding and Evans, 2002; Magnússon *et al*., 2007; Evans, 2009; Bennett *et al*., 2010; Magnússon *et al*., 2012, 2014). This moraine comprises two prominent ridges, the Kviarmýrarkambur (150 m a.s.l.) on the southern side of the glacier and Kambsmýrarkambur (129 m a.s.l.) to the north. The moraine is breached at several points, the largest of which allows the Kviá to drain the extensive proglacial to supraglacial lake which partially fills the area between the glacier and the moraine ridge (Figures 1b and c). Since its Little Ice Age maximum (c. 1900 AD) when the glacier fully occupied the moraine ridge, Kvíárjökull has retreated leaving a complex sequence of landforms and outwash sediments (Evans *et al*., 1999; Evans, 2009; Bennett *et al*., 2010; Bennett and Evans, 2012). Bennett and Evans (2012) concluded that this recession occurred in two stages: an early phase of active, temperate recession recorded by push-moraines and lateral moraines and unconfined proglacial meltwater drainage; and a later phase of incremental stagnation and pitted outwash reflecting the increasing topographic constraints imposed by the enclosing moraine ridge and the importance of the overdeepening as a depo-centre. Currently the lower reaches of Kvíárjökull can be divided into two distinct areas; a highly crevassed, topographically higher northern-side with a prominent debris-rich medial moraine on its surface; and a smoother, low-lying area to the south which is pockmarked by moulins linked to an active englacial drainage system (Bennett *et al*., 2010; Bennett and Evans, 2012; further new details also presented below).

During much of the twentieth century Kvíárjökull largely underwent a phase of steady retreat (Sigurðsson, 1998; Evans *et al*., 1999; Sigurðsson *et al*., 2007; Einarsson and Sigurðsson, 2015). However, in the 1980's and 1990's, similar to a number of other Icelandic glaciers (e.g. Falljökull, Sólheimajökull, Hyrningsjökull), Kvíárjökull underwent a period of readvance (Sigurðsson *et al.*, 2007; Hannesdóttir *et al*., 2015) coinciding with the formation of a large ice-cored, controlled moraine (Evans *et al*., 1999; Evans, 2009) which currently mantles parts of the central and northern margins of the glacier (see Figures 1c and d). In the past two decades, however, many Icelandic glaciers have entered a phase of accelerated retreat (Sigurðsson *et al.*, 2007), potentially due to increased mass balance sensitivity set against a backdrop of warmer summers and milder winters. At Kvíárjökull this retreat has been dominated by downwasting rather than lateral retreat (Bennett and Evans, 2012). However, during the winter of 2013-14 the northern margin of Kvíárjökull readvanced (see Einarsson and Sigurðsson, 2015), resulting in not only the steepening of this margin (Figures 1d, 8 and 9), but also the marked reduction in the size of an adjacent glacial lake and the formation of an ice-cored push-moraine composed of unconsolidated sand and gravel (Figure 9a). Mapping of the position of the large ice-cored esker which mantles the northeast margin of Kvíárjökull (Figure 1), using the aerial (2003, 2014) photography (Figure 6) and LiDAR (2010, 2014) imagery (Figure 8), indicates that the northeast margin of the glacier moved forward by 200-250 m. Furthermore the elevation change model generated using the 2010 and 2014 LiDAR imagery clearly indicates that the surface elevation of the northeastern frontal margin of Kvíárjökull increased by between 20 and 40 m (Figure 8). Importantly, no clear evidence of this advance has been recognised at the surface on the southern side of the glacier.

Structural architecture of Kvíárjökull

Detailed mapping of the structures exposed on the surface of Kvíárjökull has enabled the identification of a series of structural domains (Figures 2, 3, 4, 5, 6 and 10; Table 1). This approach has revealed that the structural architecture of the glacier comprises a central corridor of elongate to lobate domains along the central axis of the glacier, enclosed within lateral marginal zones composed of several relatively large domains (Figures 2b and 10a). The dominant structures identified in different parts of the glacier and their interpretation are summarised in Table 1, and described in detail below.

The brittle fractures defining all the structural domains cross-cut and locally offset a well-developed, gently to moderately up-ice dipping banding. Although they appear laterally extensive (up to over 100 m in length) on the aerial photographs, on the glacier surface the individual fractures can be seen to typically comprise several closely spaced, relatively straight, steeply inclined to vertical sections (less than 1.0 m, to over 10 m long), the propagating tips of which either overlap or are linked by short curved fracture planes. The banding within the glacier comprises alternating layers of clean (debris-free) and darker ice, the latter containing disseminated fine-grained (silt- to sand-grade) debris (Figure 11). Although at a distance the banding appears well-defined (see Figure 9), the margins of the individual bands (0.1 to 2 m thick) are in fact diffuse (see Figure 11) and gradational over several centimetres. On the surface of the glacier the banding is highlighted by the concentration of fine detritus released due to melting. This banding has been previously interpreted as ogives or Forbes bands (Swift *et al*., 2006; Bennett and Evans, 2012).

Close to the front of Kvíárjökull the banding is truncated and offset by a series of gently to moderately, up-ice dipping (15°-40°) thrusts (Figures 11a and b) which can be traced laterally across the surface of the glacier (Figure 6). The SE-directed sense of displacement of the banding across the thrusts is consistent with these brittle structures having formed in response to compression associated with the forward motion of the glacier (Figures 11a and b). Rare, tight, asymmetrical SE-verging folds were also observed to deform the banding (Figure 11c). Although clearly developed within the lateral marginal zones of Kvíárjökull, the banding and thrust faults are less apparent within the central axial zone where they appear to have been largely obscured (or even overprinted) by the intensity of the relatively later brittle fracturing.

Two prominent bedrock outcrops on the northern side of Kvíárjökull result in a marked narrowing of the glacier (Figures 2, 3, 4 and 10) and locally affect the pattern of fracturing (see Figures 2b and 3). These bedrock promontories, or their extensions beneath the ice, are likely to have formed the source of the detritus feeding the medial moraine observed on the surface of Kvíárjökull (see aerial photograph; Figure 2a). This medial moraine is marked by a thin band of debris which first appears down-ice of the upper (relative to the glacier margin) of the two bedrock outcrops, widening dramatically in the lower reaches of Kvíárjökull where it partially obscures the underlying ice.

Icefall

The domains identified towards the base of the icefall (Domains 16, 17, 18; Figures 2b, 3 and 10a; Table 1) are characterised by a series of arcuate to irregular (folded), transverse, convex down-ice, open crevasses and normal faults formed as a result of the ice-flow-parallel extension associated with the glacier descending from its source area (see Figure 1b). In Domains 18 and 17 these transverse crevasses are folded by a series of open, buckle-like folds with the axial traces of these folds occurring parallel to ice-flow (Figures 2 and 3). In Domain 17 and, to a lesser extent, Domain 16, these arcuate structures are cross-cut by a set of sigmoidal, en-echelon tension fissures defining a wide (c. 100 to 120 m) dextral (right-lateral) shear zone aligned parallel to ice-flow (Figures 2, 3 and 10), as well as a set of relatively short (10 to 30 m long) longitudinal (flow-parallel) fractures and a smaller scale set of Reidel (dextral) shears orientated at c. 30°-40° to the axis of the glacier and defined by S-shaped, closed fractures (Figures 2, 3 and 10a).

Southern lateral margin

The zone along the southern lateral marginal of Kvíárjökull comprises a series of elongate domains (Domains 1, 21, 26; Figures 2b,4 and 5; Table 1) which become progressively wider towards the terminus of the glacier (Figure 10a). In the upper part of the glacier this zone is characterised by several sets of cross-cutting fractures orientated at a high-angle to the direction of flow (see rose diagram for Domain 21; Figure 2b). For example, the southeast-end of Domain 21 is dominated by a set of straight to weakly curved fractures orientated at approximately 40°-50° to the glacier margin and antithetic to the flow direction of the ice, and therefore represent chevron crevasses resulting from lateral shear stresses at the glacier margin (Sharp *et al*., 1988; Benn and Evans, 2010; Colgan *et al*., 2016). Further down-ice, however, the pattern of crevassing is dominated by well-developed arcuate (convex down-ice) steeply inclined to subvertical, open to closed fractures (Domain 26; Figures 2b and 4). These arcuate, hook-like structures probably developed in response to a combination of lateral shear stresses and longitudinal compressive stresses imposed by the forward motion of the glacier (Benn and Evans, 2010). Comparable curved crevasses were described by Sharp *et al*., (1988) within marginal shear zones of the Variegated Glacier in Alaska.

In Domain 26 (Figures 2b and 4) the hook-like fractures are deformed by at least one set of ENE-WSW-trending dextral (right-lateral) brittle shear zones (typically 20-60 m in width, but up to 100 m wide). These shear zones dissect and apparently reactivate the earlier fractures to form a series of short (10-50 m long), open, sigmoidal to arcuate, en-echelon tension fissures (Figure 12a; also see Figure 2). The margins of the shear zones occur both at an angle (10° to 20°) (R-type Reidel shears; Figure 10b) and parallel to flow (Y-type Reidel shears; Figure 10b), and are defined by a set of relatively straight, subvertical to vertical, closed (shear-parallel) fractures. The geometry of the shear zones is consistent with them having formed in response to a right-lateral (dextral) strike-slip regime imposed by ESE/SE-directed flow of ice along the axis of the glacier. Large-scale tension gashes and Reidel shears have been described by Herbst *et al*. (2006) from the Pasterzenkees glacier in Austria where they are developed in response to shear along the margins of the glacier. Reidel shears have also been reported defining shear zones that separated individual flow units within the glacier (Herbst *et al*., 2006).

Domain 1 of the southern lateral margin occupies the relatively low-lying area immediately adjacent to the southeast-end of the glacier (Figures 2, 5, 6 and 10a). The relatively smooth surface of the ice within this domain is pock marked by a number of large moulins (Figures 1a, 1b, 2 and 5) which are linked to an active englacial drainage system. Three main fracture sets have been recognised within Domain 1: (i) vertical to subvertical, radiating, convex down-ice fractures; (ii) a set of well-developed, WNW-ESE-trending, vertical to subvertical, laterally extensive (100-300 m) longitudinal (flow-parallel) features; and (iii) arcuate, up-ice dipping, ESE/SE-directed thrusts which offset the banding within the ice (Figures 2b and 3). Thrusting is more common within Domain 1 (see Figure 6), indicative of increased compressional flow toward the glacier snout (e.g. Hambrey and Huddart, 1995; Hambrey and Dowdeswell, 1997; Glasser *et al*., 1998; Hambrey *et al*., 1999; Murray *et al*., 2000) and/or in response to flow against a reverse slope (e.g. Sharp *et al*., 1993) (see below). Fracture sets (i) and (ii) are however dominant, resulting in a marked bimodal distribution of the data on the rose diagrams plotted for this domain (see Figures 2 and 6). The longitudinal fractures are more closely spaced and more numerous towards the centre of the glacier (Figure 2b), where they offset the banding within the ice (where apparent) recording a consistent right-lateral (strike-slip) sense of displacement (Figure 6). However, adjacent to the northern margin of Domain 1 the longitudinal fractures also show evidence of both normal and reverse movement (downthrown to the N/ENE) with displacements of between 10 and 40 cm (Figures 13b and c). The resultant fault-scarps are sharp (i.e. very little modification due to surface melting) suggesting that dip-slip movement had occurred recently or was ongoing.

Also present within Domain 1 are a number of NE-SW-trending (see rose diagram; Figure 2), moderately down-ice dipping (30°-50°) reverse faults (Figure 14). These compressional structures locally form a wide (up to 15-20 m) fault zone which separates the main low-lying area of Domain 1 from an upthrown, topographically higher (1-2 m) block which extends to the glacier margin (Figure 14a; also see Figure 1b). The fault-scarps marking the hanging-walls of these faults (Figure 14a) are sharp (angular) indicative of recent/active fault movement.

All of the GPR profiles from Domain 1 (Figure 7) reveal that the bed of the glacier is marked by a continuous or semi-continuous reflector at a depth of up to 120 m beneath the surface (Figure 7c). Interpolation of the glacier bed elevation beneath Domain 1 shows an overdeepened basin reaching a depth of 70 m below sea level (Figure 7b). The eastern, down-ice side of the basin rises to 20 m below sea level, with slope ranging between 10° and 30°. This reverse slope is significantly steeper than the glacier surface slope in Domain 1 (c. 2.5°), suggesting that conditions favourable for glaciohydraulic supercooling may exist beneath this part of Kvíárjökull (Alley *et al*., 1998; Spedding and Evans, 2002; Spedding *et al*., 2006; Magnússon *et al*., 2007; Larson *et al*., 2010; Bennett and Evans, 2012;

Magnússon *et al.*, 2012, 2014). Glaciohydraulic supercooling is one possible process that could account for the distinct basal glacier radar facies that occurs above the glacier bed immediately up-ice from, and lapping onto, the reverse slope (Figure 7c). A strong, down-ice dipping reflector can be seen at the eastern-end of Line 12 (Figures 7a, c and d), from approximately 5 m below the ice surface. This reflector appears to offset a second, up-ice dipping feature which is displaced upwards on the eastern side (Figure 7d). Both reflectors are of reversed polarity, indicating a higher dielectric permittivity and lower wave velocity, suggesting that that they are water-filled fractures. The down-ice dipping reflector is interpreted as the subsurface extension of the prominent reverse fault observed on the glacier surface, and forms the up-ice margin of an up-thrown block of ice which extends to the glacier margin (Figure 14). Other features observed in the GPR profiles from the glacier include moulins, characterised by 'ringing' of the radar data, and probable englacial conduits marked by distinct strong reflectors with polarity reversals (Figure 7c).

Northern lateral margin

The zone along the northern margin of Kvíárjökull comprises a small number of elongate domains (Domains 9, 10, 11; Figures 2, 4, 5 and 10; Table 1) characterised by NE-SW trending fractures orientated at c. 90° to the axis of the glacier (Figure 3). This dominant fracture set is locally deformed by a series of sinistral (left-lateral) shear zones (Domain 11; Figures 2, 4, 10 and 12b) defined by en-echelon, sigmoidal, open tension fissures (Figure 12b). The geometry of these steeply inclined to subvertical brittle shear zones (c. 10 to 50 m wide) is consistent with their formation in response to strike-slip imposed by SE-directed ice-flow along the axis of the glacier. In the upper part of Kvíárjökull the shear zones occur parallel to ice-flow (Figures 2, 4 and 10). However, further down-ice (southern-end of Domain 11 and Domain 9; Figure 2b) they are orientated oblique (c. 20°-30°) to both the direction of flow and the glacier margin (Figures 2, 4 and 10) and are interpreted as R-type Reidel shears (Figure 10b).

Close to the southeastern-end of Kvíárjökull, the northern lateral marginal zone is separated from the remainder of the glacier by a prominent fault zone (Figure 9b and c). Movement along a number of steeply inclined to subvertical brittle fractures within this fault zone result in marked changes in the orientation and dip of the banding in the ice (Figure 9c). However, when traced laterally (up-ice) this complex fault zone becomes less apparent.

Central zone

The central zone of Kvíárjökull comprises a series of lobes linked by a laterally continuous axial zone of highly fractured ice linking the icefall to the piedmont lobe (Figures 2, 4 and 10; Table 1). The lobes form highly crevassed topographic highs on the glacier surface and exhibit a close spatial relationship to the marked constrictions caused by the two prominent bedrock outcrops on the northern side of the glacier (Figures 2, 4 and 10). The size of the lobes increases and their shape becomes more elongate down-ice. Higher in the glacier (e.g. Domain 19; Figures 2, 3 and 10) they comprise a set of arcuate fractures (convex down-ice) developed approximately transverse to flow and which mimic the shape of the lobe. These arcuate structures are deformed by relatively wide (50-100 m) dextral (right-lateral) shear zones defined by flow-parallel and associated sigmoidal en-echelon (closed) fracture sets (e.g. Domains 19 and 20; Figures 2, 3 and 10). In contrast, the fractures within a larger lobe formed further down-ice are predominantly flow-parallel and cross-cut by a series of open NNW-ESE-trending crevasses and brittle shear zones (Domains 24 and 25; Figures 2, 4 and 10). The shear zones (typically 20-60 m in width; but up to 100 m across) once again record a dextral (right-lateral) sense of shear and are defined by a series of short (10-50 m long), open, en-echelon tension fissures (Figure 10). They are aligned both parallel (Y-type Reidel shears; Figure 10b) and oblique (20°-40°) to flow and glacier margin (R-type Reidel shears; Figure 10b) with the dextral shear sense recorded by these structures being consistent with the overall ESE/SE-directed movement of the glacier (see Figures 10a and b).

The largest lobe within the central corridor of Kvíárjökull is represented by Domain 27 and corresponds to a topographically higher, highly crevassed area of the glacier immediately up-ice of the low-lying area of Domain 1 (see satellite imagery; Figure 2a). The approximately NW-SE-trending (see rose diagram; Figure 2b) open crevasses which define this domain form a radiating or fan-like pattern. The apparently laterally continuous arcuate fractures are in detail composed of a series of shorter, relatively straight segments. These segments are offset or “stepped” to form the resulting curved fracture, or linked by a set of smaller-scale, slightly oblique structures. The radiating pattern is cross-cut by a set of younger, short (c. 20-30 m long), NE-SW trending fractures orientated orthogonal to flow. These open crevasses occur in two distinct areas (Figure 2b) and are interpreted as the record of extension occurring parallel to flow. Radiating or fan-like crevasses typically develop toward the snout of a glacier, recording longitudinal compression and lateral expansion of the ice as the confining valley begins to widen (e.g. Variegated Glacier, Alaska, Lawson *et al*., 1994; Fox Glacier, New Zealand Appleby *et al*., 2010). However at Kvíárjökull, Domain 27 is located on the southern-side of the glacier, approximately 1-2.5 km up-ice from the present glacier margin (see Figures 2 and 4), and so is unlikely to have formed as a result of the spreading of the ice within the developing piedmont lobe. The formation of a radiating crevasse pattern higher in a glacier has recently been described at Falljökull (SE

Iceland) where it is associated with lateral expansion of the active upper part of the glacier as it overrides the slow moving/stagnant lower section (Phillips *et al*., 2014).

The highly crevassed, relatively narrow, axial zone to Kvíárjökull (Domains 6, 12, 13 and 15; Figures 2, 3, 4 and 10b) comprises a set of longitudinal (flow-parallel) structures and arcuate (convex down-ice), open to closed fractures developed transverse (i.e. orthogonal) to flow (Figures 2 and 4); the latter suggests that changes in the flow regime down the axis of the glacier resulted in the switching between localised extension (open) and compression (closed). The transverse fractures are locally deformed by a series of flow-parallel, longitudinal fractures and dextral brittle shear zones (Figures 4 and 10a) interpreted as Y-type Reidel shears (Figure 7b). The elongate domains defining the axial zone to Kvíárjökull clearly cross-cut and truncate the relatively earlier developed teardrop-shaped lobes (Figures 2b and 7b).

Northeast frontal margin

Close to the front of Kvíárjökull the central zone can be traced (down-ice) into a triangular shaped area of highly crevassed, partially debris covered ice which occupies the entire northeastern-side of the glacier (Figures 2, 5, 6 and 10; Table 1). This area can be subdivided into two: a relatively poorly exposed, largely debris covered northern subzone in which the dominant ice-flow parallel fractures are deflected into a ENE-WSW to NE-SW orientation (Domains 7 and 8; Figures 2, 5 and 6); and a structurally more complex southern subzone comprising a series of arcuate, S-shaped domains (Domains 2, 3, 4 and 5; Figures 2, 5 and 6; Table 1) characterised by well-developed, closely spaced curved, open to closed, steeply inclined fractures. The asymmetrical shape of the domains and fractures within the southern subzone yields an overall sense of shear (dextral) towards the E/ESE (Figures 6 and 10c). On the 2014 satellite image the arcuate fractures within this shear zone offset both the banding (where apparent) and other small-scale vertical to subvertical structures present within the ice, recording a right-lateral sense of strike-slip displacement towards the NE (Figure 6). The elongate NE-SW-trending ridge-like blocks of ice bound by these strike-slip faults are locally deformed by subvertical, open, sigmoidal tension fissures which also record a NE-directed (dextral) sense of shear (Figures 15a to d). These small-scale features are thought to have developed as the elongate blocks of ice moved past one another as they accommodated the strike-slip occurring within the much larger (c. 200-250 m wide) dextral shear zone (Figure 10c).

The boundary between the dextral shear zone and Domain 1 to the south is gradational over several tens of metres, with the strike-slip displacement being taken up by the laterally extensive flow-parallel fractures (Figures 5, 6 and 10). This not only offsets the banding within the ice (see previous section) but also resulted in ductile shearing along the longitudinal fractures, leading to the development of a rarely preserved asymmetrical S-C-fabric (Figure 15e). In contrast to the southern boundary, the northern limit of the main shear zone is marked by an approximately WSW-ESE-trending domain characterised by well-developed small-scale shears (20-50 m wide) (Domain 8a; Figures 2b, 5 and 6), interpreted as Y and R-type Riedel shears.

The GPR profiles from the foreland beyond the northeastern margin of the glacier reveal that the structurally lower part of the sedimentary sequence is deformed by a number of structures interpreted as open, asymmetrical folds and thrusts, and are indicative of ice-push towards the northeast (Figure 7e). Some of the structures are clearly truncated by the horizontally stratified outwash sediments which form the upper part of the sequence and are now vegetated on the surface. These GPR profiles are located beyond an ice-cored moraine complex, but are inside the large Holocene moraine ridge that was occupied during the Little Ice Age. They indicate that earlier episodes of ice-push at the northeast glacier margin have occurred since overall retreat from the Little Ice Age maximum position.

Interpretation of the structure of Kvíárjökull

It is clear from the above detailed description that Kvíárjökull is internally structurally complex (see Figures 2, 3, 4, 5 and 10, and Table 1) with the pattern of fracturing reflecting changes in the stress regime within the glacier as it moves from its accumulation zone via the icefall, through the confines of a valley, finally forming a low-gradient piedmont lobe at its margin. In the following sections this structural complexity is interpreted in terms of a model of concentrated axial glacial flow. Historical aerial photographs and satellite imagery are used to investigate how this pattern of ice flow has evolved since the 1940s to present.

Concentrated axial glacier flow

The structurally complex nature of Kvíárjökull is inconsistent with it advancing down the enclosing valley as a single, predominantly integrated or plug-type flow. The simplest interpretation of the internal structural architecture of this glacier is in terms of a central corridor of highly crevassed ice and elongate to lobate domains enclosed by two lateral marginal zones (Figure 10 and Table 1). The cross-cutting relationships between these components indicate that deformation within this central corridor largely post-dates that imposed on the ice along the margins of the glacier. The central corridor links the icefall to the structurally more complex zone marking the northeast-side of the snout. The northern margin of this corridor is marked by a medial moraine which emerges onto the surface of

Kvíárjökull down-ice of a prominent bedrock outcrop located on the northern-side of the glacier (Figures 1b and 2a). The recent landform record and changes in surface elevation (Figure 8) on the northeastern-side of Kvíárjökull indicates that it is still active with an advance during the winter of 2013-14 resulting in the formation of an ice-cored push-moraine (Figure 9a). In contrast to its northeast-margin, the positon of the margin on the low-lying southern-side of the glacier has remained in approximately the same position (see air photographs on Figure 16) and lacks any obvious landform record indicative of active retreat. This suggests that the southern-side of the glacier may be either very slow moving or even stationary, leading to the conclusion that the two sides of Kvíárjökull are acting independently (c.f. Bennett, 2010). Consequently, the central corridor of Kvíárjökull is considered to have acted as the primary focus for the recent flow supplying ice from the source area on Öræfajökull, via the icefall, to the northeast-margin of the glacier (Figure 10).

The elongate domains identified within the icefall (Figures 2b and 10a; Table 1) are interpreted as individual flow units with the open transverse crevasses representing extensional faults formed during gravitational failure and rotational-slip of the descending blocks of ice (seracs). The flow-parallel, right-lateral (dextral) shear zones and longitudinal fractures in this part of the glacier formed in response to differential movement between the individual flow units. Cross-cutting relationships between the flow units (see Figure 10a) suggest that the focus of activity has migrated across the icefall as different parts of the glacier destabilised and accelerated. The passage linking the icefall to the remainder of Kvíárjökull is narrow due to the presence of the prominent bedrock outcrop on its northern side (see Figures 2, 3 and 10), resulting in compression and folding of the seracs as they entered and moved through this constriction. Similar folding of seracs separated by convex down-ice transverse crevasses has been described by Lawson (1996) from the upper zone of the Variegated Glacier in Alaska were ice descending the ice-fall enters into the confines of the valley.

Down-ice, Kvíárjökull narrows once again due to the presence of a second prominent bedrock outcrop on the northern side of the glacier (see Figures 2, 4 and 10). Both of these bedrock constrictions may have influenced the volume and/or rate at which ice was fed to the lower reaches of glacier. The elongate lobes of ice within the central corridor of the glacier (see Figure 10a) are interpreted as individual flow units of ice that move independently or "pulsed". The constrictions caused by the bedrock outcrops are thought to extend as bedrock highs beneath the glacier, restricting flow and leading to the temporary storage/build-up of ice immediately up-ice of these features. This temporary accumulation of ice will eventually reach a critical volume where it overwhelms the bedrock high/constriction, migrating further down-ice as an elongate lobe. Volumetrically smaller flow units may run out of forward momentum and cease partway down the glacier. The increasing size of the lobes down-glacier suggests that either the size (volume) of these pulses of ice changed over time, or that they are capable of incorporating/entraining ice from older flow units and/or the margins of the glacier as they move down-ice.

Importantly the lobes formed by the individual flow units occur on the southern-side of the central corridor and are truncated by the axial zone which is interpreted as forming the main conduit feeding ice from the icefall to the glacier margin. This geometry may result from the bedrock outcrops on the northern-side of the glacier deflecting flow towards its southern side. The overall ESE/SE-directed movement of these proposed lobate pulses led to shearing of the ice within the southern lateral margin of Kvíárjökull and the development of dextral (right lateral) Y and R-type Reidel shears (Figures 10a, 10b and 12a). The individual lobes also form topographically higher areas of the glacier surface (see Figures 1b, 1c and 8) suggesting that they may partially override the slow moving or static ice at the glacier margin. As the active lobe overrides this marginal ice it will emerge from the confines of the central corridor of the glacier allowing it to spread laterally with the combination of lateral extension and forward compression, leading to the development of a radiating/splaying crevasse pattern (e.g. Domain 27; Figures 2, 4 and 10a). The narrow shear zones deforming the earlier formed fracture sets within the lobes may result from either shearing imposed by the passage of later pulses of ice as they migrate down the axis of Kvíárjökull, or the partitioning of deformation into increasingly narrower zones as the ice begins to stop moving and the flow unit “locks up”.

Close to the front of Kvíárjökull the crevasse pattern within the ice indicates that the central pattern of flow is deflected towards the northeast margin of the glacier, probably due to the presence of the low-lying area of essentially static ice on the southern-side of the snout. The periodic readvance of Kvíárjökull during the period of overall recession has resulted in the development of a series of locally ice-cored push-moraines (Figure 6a), as well as ice-marginal to proglacial thrusting and folding of the adjacent outwash sequence (Figure 4e; cf. Bennett and Evans, 2012). However, the main response to the delivery of a pulse of ice into this part of the glacier was the thickening of the ice at the snout, leading to an increase in surface elevation (see Figures 1, 2 and 8). The thickening of the glacier snout, rather than it simply moving forward, is thought to be a consequence of the reverse slope of the bed (Magnússon *et al*., 2007, 2012, 2014) proving to be an obstruction to advance. The elevation change model constructed for the marginal zone of Kvíárjökull shows that the surface elevation of northern part of Domain 8 (Figures 2, 5 and 6) has increased by 30 to 40 m (Figure 8). The boundary between the highly crevassed “active” part of the glacier and the relatively smooth slow moving to static, low-lying area immediately adjacent to its southeastern margin is complex, comprising a wide dextral (right-lateral) shear zone and zone of closely spaced longitudinal fractures and dextral strike-slip faults (Figures 2, 10a and 10c, and Table 1). A comparison between the 2010 LiDAR imagery and 2014 high-resolution satellite imagery reveals that displacement across the shear zone led to the clockwise rotation of the ice-cored esker (Figure 6) developed close to the margin of Kvíárjökull (Figure 1b and c). Strike-slip movement across the longitudinal fractures resulted in c. 260 m of down-ice displacement of the esker between 2010 and 2014 (Figures 6 and 8). This estimate is similar to the amount of forward movement (up to 200-250 m) on the northeastern-side of Kvíárjökull measured from the aerial photographs and LiDAR imagery (Figures 6 and 8 respectively). Consequently, it is possible that the rotation and down-ice displacement of the ice-cored esker occurred during the most recent 2013-14 advance. Narrow, cross-cutting WSW-ESE-trending shears (Figures 6 and 10c) visible within the NE-active part of the glacier represent Y and R-type Reidel shears formed in response to the partitioning of deformation during the later stages and "locking up" of individual flow events. Recent dip-slip movement and localised normal and reverse displacement (downthrown to the N/ENE; Figures 13b and c) on the longitudinal fractures may reflect the initial "collapse" and downwasting during retreat of the glacier from its minor readvance limit represented by the 2013-14 push-moraine.

The concentration of flow along the central axis of Kvíárjökull means that the northern and southern lateral margins of the glacier have essentially been bypassed and are either static or very slow moving. Consequently, the crevasses within these lateral margins (Figures 2, 3, 4 and 10) are thought to largely record deformation associated with the much earlier "plug-like" flow of the entire glacier. The chevron and hook-like geometry of the crevasses adjacent to the southern lateral margin of Kvíárjökull is consistent with their formation in response to the combination of lateral shear stress and longitudinal compressive stress imposed during this type of flow (Sharp *et al*., 1988; Benn and Evans, 2010; Colgan *et al*., 2016). The orthogonal geometry of the fractures adjacent to the northern margin, however, may indicate either the passive rotation (towards the ESE/SE) of initial chevron crevasses during continued flow, and/or a marked change in stress regime immediately down-ice of the bedrock outcrops on this side of Kvíárjökull (see Figures 2 and 10). The geometry of the shear zones deforming the earlier developed fractures within the lateral marginal zones (dextral on the southern-side and sinistral to the north; Figures 2 and 10) is consistent with their formation in response to lateral shear imposed by ice moving down the central ice flow corridor of Kvíárjökull.

The radiating fractures and thrusts in the area immediately adjacent to the southeast-margin of Kvíárjökull (Domain 1; Figures 2, 5 and 10; Table 1) can be interpreted in terms of the deformation occurring towards the snout of the plug-like flow. The radiating fractures are a relic of a splaying crevasse pattern (Sharp *et al*., 1998; Lawson *et al*., 1994; Appleby *et al*., 2010). However, on the NE-side of Kvíárjökull this relatively simple "fan-like" architecture is replaced by the more complex marginal zone associated with the later concentrated axial flow (Figures 2 and 10). Thrusting on the southern-side of the glacier is not only thought to result from increased compressional flow toward the snout (c.f. Hambrey and Huddart, 1995; Hambrey and Dowdeswell, 1997; Glasser *et al*., 1998; Hambrey *et al*., 1999; Murray *et al*., 2000), but also due to the effects of movement against the reverse slope (c.f. Sharp *et al*., 1993) marking the down-ice side of the overdeepening located beneath this part of Kvíárjökull (Figures 7b and c).

In contrast to the northeastern "active" side of Kvíárjökull, the southeastern-side of the glacier has apparently lowered by c. 8 to10 m between 2010 and 2014 (Figure 8). This surface lowering may simply reflect increased surface melting as a result of increasingly warmer summers and milder winters. However, the surface change model shown in Figure 8 indicates that the elevation of the remainder of Kvíárjökull has increased by between 5 to 25 m over the same time period. Is it possible that ablation alone is responsible for the 8 to 10 m surface lowering of Domain 1, and that ablation and surface lowering was of the same order of magnitude across the remainder of Kvíárjökull, but was simply compensated for by the structural uplift that occurred during the readvance. An alternative hypothesis is that the southeastern-side of the glacier was lowered/depressed during the 2013-14 advance. Although there is no obvious evidence within the recent landform record on this southeast-side of the glacier, it is possible that the relatively slow moving ice within Domain 1 did in fact move forward during this readvance, potentially driven by the overriding flow-unit represented by Domain 27. As the ice on this side of the glacier moved forward it would have been driven up the reverse slope identified on the GPR profiles (Figures 7b and c). Consequently the elevation of the "leading-edge" of the block (Domain 1) would have increased as it moved up the reverse slope, leading to the formation of the topographically higher area fringing the southeastern margin of the glacier (Figures 1b, 8 and 14). The resulting rotational block movement would have led to the relative lowering of the up-ice "trailing-edge" of Domain 1 (represented by the surface lowering in this part of the glacier). The down-ice dipping reverse faults within the leading-edge of Domain 1 (Figures 7d and 14) can be interpreted as back-thrusts formed due to compression as the ice was effectively "shunted" onto the bedrock located on the down-ice side of the overdeepening beneath this part of Kvíárjökull.

Structural evolution of Kvíárjökull between 1945 and 2014

Detailed mapping of the structural architecture of the lower reaches of Kvíárjökull using a series of historical aerial photographs taken in 1945, 1964, 1980, 1998 and 2003 has revealed that the concentrated axial style of flow and focusing of forward movement on the northeastern-side of the glacier margin has been occurring for at least the last 70 years (Figure 16). Consequently, this style of flow it is not a recent adaptation in glacier dynamics in response to climate change.

Figures 6 and 16 clearly demonstrate that the structural complexity of the northeastern-side of Kvíárjökull has changed over time, potentially reflecting decadal changes in the volume of ice making its way through the glacier system to its snout. In 1945 the "active" northeastern-side of the glacier is relatively wide and the structure of the ice dominated by a radiating fan-like fracture pattern, cut by a number of wide (100 to 300 m), steeply inclined dextral shear zones (Figure 16a). Crevasses within the axial zone which fed ice to the active margin are primarily longitudinal, ice-flow parallel structures. In 1964, however, the earlier radiating fracture pattern is absent and has been replaced by several sets of cross-cutting crevasses (Figure 16b). Between 1945 and 1964 the central axial zone of Kvíárjökull is in the order of 400 to 600 m across and composed of a small number of elongate domains (Figures 16a and b). However, in 1964 the longitudinal fracture pattern has been replaced by a complex pattern of cross-cutting fractures (Figure 16b).

The structural architecture of Kvíárjökull in 1980 marks an apparent return to an overall fan-like radiating crevasse pattern with the active zone on the northeast-side of the glacier. The cross-cutting relationships between the individual domains are interpreted as recording the sequential emplacement of a series of fault-bound blocks of ice against the relatively immobile southeast-side of the glacier (Figure 16c). Bennett (2010) and Bennett and Evans (2012) concluded that during the period between 1980 and 1998 there was a marked increase in surface elevation of the northeastern margin of Kvíárjökull. This change in elevation, coupled with the marked increase in the structural complexity of this part of the glacier is consistent with an increase in the volume of ice being supplied to this part of the snout. Up-ice of the structurally complex active marginal zone the architecture of the central part of Kvíárjökull has also changed with a marked widening of the axial zone and possible initial development of the lobate pattern within this area of the glacier (Figure 16c).

The structure of Kvíárjökull in 1998 records a marked narrowing of the active zone and appearance of the large ice-cored controlled moraine along the northeast margin of the glacier (Figure 16d). The area of static ice on the southeastern-side of the glacier has increased, possibly as a result of the fault-bound blocks of ice emplaced into the southern margin of the active zone during the 1980s becoming accreted onto the northern margin of this inactive block. The structural complexity of the central zone of the glacier has further increased with the elongate lobes recording a weak southeast-directed radiating pattern of ice movement. These lobes represent individual flow units which failed to migrate to the snout. In 2003 the structure of the axial zone had once again narrowed to form a relatively linear corridor composed of a small number of highly elongate domains. The arcuate fracture pattern within the relatively narrow active zone suggests that ice is once again being deflected north-eastwards by the area of static ice on the southeast-side of the glacier. The structural architecture of Kvíárjökull in 2003 is comparable to that in 1945 with this relatively simple pattern possibly representing periods of "quiescence" when only small volumes of ice were being transferred from the accumulation zone on Öræfajökull via the axial zone to the active zone on the northern side of its snout (also see video supplementary publication).

Although the structural architecture of Kvíárjökull has changed over the past 70 years reflecting changes in the volume of ice being channelled along its axis to the snout, the position of its margin has remained constant (compare the aerial photographs on Figure 16). This is consistent with the conclusion of Bennett and Evans (2012) that retreat at Kvíárjökull has largely been dominated by downwasting rather than lateral retreat, possibly as a result of the overdeepening beneath its margin.

Pulsed ice flow to explain the structural evolution of Kvíárjökull

The large-scale changes in the structure of Kvíárjökull clearly reflect major changes in its dynamics and the volume of ice being supplied from the accumulation zone to its active northeastern margin. Similarly the lobate architecture of parts of the central axial zone which fed ice to the margin is also consistent with the migration of individual flow units or "pulses" of ice through the glacier. As noted above, the change in the structural complexity of Kvíárjökull between 1945 and 2014 reflects decadal changes in the volume of ice passing through the glacier system. The results of the mapping indicate that the period between 1980 and 1998 potentially represents a period of increased activity which culminated with the formation of a large, arcuate ice-cored moraine along the northeast margin of Kvíárjökull (see Figure 16).

A simple time-lapse animation created from the Landsat satellite images for the period 1985-2016 has revealed some interesting aspects in relation to the changing dynamics of Kvíárjökull (see video supplementary material): (i) There was a period of relatively faster ice flow between 1985 and 1990, and a small "pulse" or "jump" in forward motion in between 1990 and 1998. This decade also saw the emergence of the arcuate controlled moraine on the surface of Kvíárjökull and its transportation to the ice margin, eventually reaching the margin in 1998-1999. Furthermore during this period of increased activity the medial moraine is displaced towards the northeast-side of the glacier; (ii) The period between 1999 and 2002 is characterised by relatively slow ice movement; (iii) This was followed by ice margin stagnation between 2002 and 2013, coupled with generally slow movement of ice up-glacier; and (iv) The end of 2013 and beginning of 2014 is marked by a an apparently short lived (possibly a few months) change in flow or "mini-surge" which resulted in the rapid advance of the northeastern margin of Kvíárjökull. Comparable short duration (i.e. several weeks) "mini-surges" have been recognised in several other glaciers; for example, on the Ryder Glacier (Greenland) at the end of the 1995 melt season (Joughin *et al*., 1996) and have been identified in neighbouring Breiðamerkurjökull (Boulton, 1986; Boulton *et al*., 2001).

It is apparent from the time-lapse animation that the dynamics of Kvíárjökull are in fact characterised by periods or pulses of increased ice flow separated by periods of "quiescence" (see video supplementary material). This pulse-like activity occurs on a decadal time scale with the period of increased flow between the mid-1980s and mid-1990s coinciding with the increase in the structural complexity of the glacier.

Conclusions

A detailed structural glaciological study coupled with ground penetrating radar and aerial photogrammetry surveys have demonstrated that recent flow within Kvíárjökull in SE Iceland has been concentrated within a narrow corridor located along its central axis. This central corridor is responsible for feeding ice from the accumulation zone on the south-eastern side of Öræfajökull via an icefall, down through a steeply incised valley to a structurally more complex zone marking the northeast-side of the glacier snout. The recent landform record and changes in surface elevation on this side of the glacier indicate that it is still active and advanced during the winter of 2013-14.

The active central corridor comprises a series of elongate lobes of ice linked by a laterally continuous zone of highly fractured ice characterised by prominent flow-parallel crevasses. The lobes are interpreted as individual flow units of ice that move independently or "pulse" with volumetrically smaller flow units stalling partway down the glacier. The increasing size of the lobes down-glacier suggests that either the size (volume) of these pulses of ice changed over time, or that they incorporated/entrained ice from older flow units and/or the margins of the glacier as they move down-ice. The central corridor is enclosed by two lateral marginal zones in which the ice is either stationary or very slow moving. The cross-cutting relationships between these components indicate that deformation within the central corridor largely post-dates that imposed on the ice along the margins of the glacier. Consequently the marginal zones are being bypassed by more recent ice flow with the crevasses within these lateral margins being interpreted as largely recording deformation associated with much earlier “plug-like” flow of the entire glacier.

Continued southeast-directed movement of ice down the central corridor led to shearing within the lateral margins and the development of Reidel shears which deformed the earlier developed structures. The individual lobes within the central corridor form topographically higher areas on the glacier surface suggesting that they may partially override the slow moving ice at the margin. Close to the front of Kvíárjökull the crevasse pattern within the ice indicates that the central pattern of flow is deflected towards the northeast, probably due to the presence of a low-lying area of stationary ice on the southern-side of the snout. The boundary between this static ice and the active corridor is marked by a number of ice flow-parallel strike-slip faults and a prominent dextral shear zone which resulted in the clockwise rotation and dissection of an ice-cored esker exposed on the glacier surface.

Detailed analysis of the structural architecture of the lower reaches of Kvíárjökull since the 1940s reveals that the concentrated axial style of flow has been occurring for some considerable time and is not a recent adaptation in glacier dynamics in response to climate change. In contrast, the changes in the structural complexity of the glacier are thought to reflect decadal changes in ice volume passing through the ice fall driven by changes in its mass-balance. Changes in the structural complexity of the active northeastern-side of Kvíárjökull are thought to reflect decadal changes in the volume of ice making its way through the glacier system to its snout. A time-lapse animation for the period 1985-2016 reveal that Kvíárjökull underwent a period of relatively fast ice flow between 1985 and 1990, and small “pulses” in forward motion in between 1990 and 1998, and at the end of 2013 and beginning of 2014. These periods of fast ice flow are separated by periods of “quiescence” when the margin stagnates and flow is confined to the upper part of the glacier. This suggests that the concentrated style of axial glacier flow identified within Kvíárjökull has affinities with the individual flow units which operate within pulsing or surging glaciers.

Acknowledgements

This paper is published with the permission of the Executive Director of the British Geological Survey, Natural Environmental Research Council. Keith Westhead is thanked for his comments on an earlier version of this paper. David Graham and two anonymous reviewers are thanked for their constructive reviews.

References

Alley, R.B., Lawson, D.E., Evenson, E.B., Strasser, J.C. and Larson, G.J. 1998. Glaciohydraulic supercooling: A freeze-on mechanism to create stratified, debris-rich basal ice: II. Theory. *Journal of Glaciology*, **44,** 563–569.

Allen, C.R., Kamb, W.B., Meier, M.F. and Sharp, R.P. 1960. Structure of the Lower Blue Glacier, Washington. *The Journal of Geology*, **68,** 601-625.

Appleby, J.R., Brook, M.S., Vale, S.S. and MacDonald-Creevey, A.M. 2010. Structural glaciology of a temperate, maritime glacier: Lower Fox Glacier, New Zealand. *Geografiska Annaler*, **92A**, 451–467.

Bennett, M.R. 2003. Ice streams as the arteries of an ice sheet: their mechanics, stability and significance. *Earth Science Reviews* **61,** 309-339.

Bennett, M.R., Huddart, D. and Waller, R.I. 2000. Glaciofluvial crevasse and conduit fills as indicators of supraglacial dewatering during a surge, Skeiðarárjökull, Iceland. *Journal of Glaciology*, **46,** 25-34.

Bennett, G.L. 2010. Assessing glacier retreat and landform production at the `debris-charged' snout of Kvíárjökull, Iceland. Durham theses, Durham University. Available at Durham E-Theses Online: http://etheses.dur.ac.uk/110/.

Bennett, G.L. and Evans, D.J.A. 2012. Glacier retreat and landform production on an overdeepened glacier foreland: the debris-charged glacial landsystem at Kvíárjökull, Iceland. *Earth Surface Process and Landforms*, **37,** 1584–1602.

Bennett, G.L., Evans, D.J.A., Carbonneau, P. and Twigg, D.R. 2010. Evolution of a debris-charged glacier landsystem, Kvíárjökull, Iceland. *Journal of Maps* **2010**. 40–76.

Benn, D.I. and Evans, D.J.A. 2010. *Glaciers and Glaciation*. Arnold, London 802 pp.

Benediktsson, Í.Ö., Ingólfsson, Ó., Schomacker, A. and Kjær, K.H. 2009. Formation of submarginal and proglacial end moraines: implications of ice-flow mechanism during the 1963–64 surge of Brúarjökull, Iceland. *Boreas*, **38,** 440–457.

Benediktsson, Í.Ö., Schomacker, A., Lokrantz, H. and Ingólfsson, Ó. 2010. The 1890 surge end moraine at Eyjabakkajökull, Iceland: a re-assessment of a classic glaciotectonic locality. Quaternary Science Reviews, 29, 484-506.

Boulton, G.S. 1986. Push moraines and glacier contact fans in marine and terrestrial environments. *Sedimentology*, **33,** 677–698.

Boulton, G.S., Dobbie, K.E. and Zatsepin, S. 2001. Sediment deformation beneath glaciers and its coupling to the subglacial hydraulic system. *Quaternary International*, **86,** 3-28.

Burke, M.J., Woodward, J., Russell, A.J., Fleisher, P.J. and Bailey, P.K. 2008. Controls on the sedimentary architecture of a single event englacial esker: Skeiðarárjökull, Iceland. Quaternary Science Reviews, 27, 1829-1847.

Cassidy et al. 2003, in: Bristow and Jol (eds.) GPR in Sediments. *Geological Society of London Special Publication,* **211,** 153-166.

Colgan, P.M., Mickelson, D.M. and Cutler, P.M. 2003. Ice marginal terrestrial landsystems: southern Laurentide Ice Sheet margin. In: Evans, D.J.A. (ed.), *Glacial Landsystems*. Arnold, London, pp. 111-142.

Colgan, W., Rajaram, H., Abdalati, W., McCutchan, C., Mottram, R., Moussavi, M.S. and Grigsby S. 2016. Glacier crevasses: Observations, models, and mass balance implications. *Reviews of Geophysics*, **54,** doi:10.1002/2015RG000504.

Dyke, A.S. and Morris, T.F. 1988. Drumlin fields, dispersal trains and ice streams in arctic Canada. *Canadian Geographer* **32,** 86-90.

Dyke, A.S., Morris, T.F., Green, D.E.C. and England, J. 1992. Quaternary Geology of Prince of Wales Island, Arctic Canada. Geological Survey of Canada, Memoir **433**.

Einarsson, B. and Sigurðsson, O. 2015. Jöklabreytingar 1930-1970, 1970-1995, 1995-2013 og 2013-2014. *Jökull*, **65,** 91-96.

Evans, D.J.A. 2009. Controlled moraines: origins, characteristics and palaeoglaciological implications. *Quaternary Science Reviews*, **28,** 183–208.

Evans, D.J.A., Archer, S. and Wilson, D.J.H. 1999. A comparison of the lichenometric and Schmidt hammer dating techniques based on data from the proglacial areas of some Icelandic glaciers. *Quaternary Science Reviews*, **18,** 13–41.

Evans, D.J., Ewertowski, M. and Orton, C. 2015. Fláajökull (north lobe), Iceland: active temperate piedmont lobe glacial landsystem. *Journal of Maps*, 1-13. http://dx.doi.org/10.1080/17445647.2015.1073185.

Evans, D.J.A., Storrar, R.D. and Rea, B.R. 2016. Crevasse-squeeze ridge corridors: diagnostic features of late stage palaeo-ice stream activity. *Geomorphology* **258,** 40-50.

Eyles, N. and Rogerson, R.J. 1978. A framework for the investigation of medial moraine formation: Austerdalsbreen, Norway, and Berendon Glacier, British Columbia, Canada. *Journal of Glaciology* **20,** 99-113.

Frappé, T.-P. and Clarke, G.K.C. 2007. Slow surge of Trapridge Glacier, Yukon Territory, Canada. *Journal of Geophysical Research*, **112,** F03S32, doi:10.1029/2006JF000607.

Glasser, N.F., Hambrey, M.J. Crawford, K., Bennett, M.R. and Huddart, D. 1998. The structural glaciology of Kongsvegen, Svalbard and its role in landform genesis. *Journal of Glaciology*, **44,** 136–148.

Glasser, N.J., Hambrey, M.J., Etienne, J.L., Jansson, P. and Pettersson, R. 2003. The origin and significance of debris-charged ridges at the surface of Storglaciären, northern Sweden. *Geografiska Annaler Series A-Physical Geography*, **85A,** 127-147.

Glasser, N.F. and Scambos, T.A. 2008. A structural glaciological analysis of the 2002 Larsen B ice-shelf collapse. *Journal of Glaciology*, **54,** 3-16.

Goodsell, B., Hambrey, M.J., Glasser, N.F., Nienow, P. and Mair, D. 2005. The structural glaciology of a temperate valley glacier: Haut Glacier d'Arolla, Valais Switzerland. Arctic, Antarctic and Alpine Research, 37, 218-232.

Hambrey, M.J. and Milnes, A.G. 1977. Structural geology of an Alpine glacier (Griesgletcher, Valais, Switzerland). *Eclogae Geologicae Helvetiae*, **70,** 667-684.

Hambrey, M.J. and Huddart, D. 1995. Englacial and proglacial glaciotectonic processes at the snout of a thermally complex glacier in Svalbard. *Journal of Quaternary Science*, **10,** 313–326.

Hambrey, M.J. and Dowdeswell, J.A. 1997. Structural evolution of a surge-type glacier: Hessbreen, Svalbard. *Annals of Glaciology*, **24,** 375– 381.

Hambrey, M.J. and Lawson, W.J. 2000. Structural styles and deformation fields in glaciers: a review. In: Maltman, A.J., Hubbard, B. and Hambrey, M.J. (eds.), Deformation of Glacial Materials. *Geological Society of London, Special Publication* **176,** 59-83.

Hambrey, M.J. and Glasser, N.F. 2003. The role of folding and foliation development in the genesis of medial moraines: examples from Svalbard glaciers. *Journal of Geology* **111,** 471-485.

Hambrey, M.J., Bennett, M.R. Dowdeswell, J.A. Glasser, N.F. and Huddart, D. 1999. Debris entrainment and transfer in polythermal valley glaciers. *Journal of Glaciology*, **45,** 69-86.

Hannesdóttir, H., Björnsson, H., Pálsson, F., Aðalgeirsdóttir, G. and Guðmundsson, Sv. 2015. Changes in the southeast Vatnajökull ice cap, Iceland, between ~ 1890 and 2010. *The Cryosphere*, **9,** 565–585.

Herbst, P., Neubauer, F. and Schöpfer, M.P.J. 2006. The development of brittle structures in an alpine valley glacier: Pasterzenkees, Austria, 1887–1997. *Journal of Glaciology*, **52,** 128-136.

Hulbe, C.L. and Fahnestock, M. 2004. West Antarctic ice stream discharge variability: mechanism, controls and pattern of grounding-line retreat. *Journal of Glaciology* **50,** 471-484.

Hulbe, C.L. and Fahnestock, M. 2007. Century scale discharge, stagnation and reactivation of the Ross ice streams, Antarctica. *Journal of Geophysical Research* **112,** doi:10.1029/2006JF000603

Huddleston, P.J. and Hooke, R.L. 1980. Cumulative deformation in the Barnes Ice Cap and implications for the development of foliation. *Tectonophysics*, **66,** 127-146.

Jennings, C.E. 2006. Terrestrial ice streams: a view from the lobe. *Geomorphology*, **75,** 100-124.

Jennings, S.J.A., Hambrey, M.J. and Glasser, N.F. 2014. Ice-flow unit influence on glacier structure, debris entrainment and transport. *Earth Surface Processes and Landforms* **39,** 1279-1292.

Jóhannesson, T. and Sigurðsson, O. 1998. Interpretation of glacier variations in Iceland 1930-1995. *Jökull*, **45,** 27-33.

Joughin, I., Tulaczyk, S., Fahnestock, M. and Kwok, R. 1996. A Mini-Surge on the Ryder Glacier, Greenland, Observed by Satellite Radar Interferometry. *Science*, **274,** 228.

Joughin, I., Tulaczyk, S., Bindschadler, R. and Price, S.F. 2002. Changes in West Antarctic ice stream velocities: observation and analysis. *Journal of Geophysical Research* **107,** doi:10.1029/2001JB001029.

Kjær, K.H., Sultan, L., Krüger, J. and Schomacker, A. 2004. Architecture and sedimentation of outwash fans in front of the Mýrdalsjökull ice cap, Iceland. *Sedimentary Geology*, **172,** 139-163.

Kamb, B., Raymond, C.F., Harrison, W.D., Engelhardt, H., Echelmeyer, K.A., Humphrey, N., Brugman, M.M. and Pfeffer, T. 1985. Glacier surge mechanism: 1982-1983 surge of Variegated Glacier, Alaska. *Science*, **227,** 469-479.

Kamb, B. and Engelhardt, H. 1987. Waves of accelerated motion in a glacier approaching surge: the mini surges of Variegated Glacier, Alaska, USA. *Journal of Glaciology* **33,** 27-46.

Kleman, J. and Glasser, N.F. 2007. The subglacial thermal organization (STO) of ice sheets. *Quaternary Science Reviews* **26,** 585-597.

Larson, G.J., Lawson, D.E., Evenson, E.B., Knudsen Ó., Alley, R.B., Phanikumar, M.S. 2010. Origin of stratified basal ice in outlet glaciers of Vatnajökull and Öræfajökull, Iceland. *Boreas*, **39,** 457–470.

Lawson, W. 1996. Structural evolution of Variegated Glacier, Alaska, U .S.A., since 1948. *Journal of Glaciology*, **42,** 261-271.

Lawson, W., Sharp, M.J. and Hambrey, M.J. 1994. The structural glaciology of a surge-type glacier. *Journal of Structural Geology*, **16,** 1447-1462.

Magnússon et al. 2007: Landslag í grennd Kvískerja í fortíð og framtíð: Niðurstöður íssjármælinga á Kvíár-, Hrútár- og Fjallsjökli. *Jökull*, **57,** 83-89.

Magnússon et al. 2012: Removing the ice cap of Öræfajökull central volcano, SE-Iceland: Mapping and interpretation of bedrock topography, ice volumes, subglacial troughs and implications for hazards assessments. *Jökull*, **62,** 131-150.

Magnússon et al. 2014: Erratum; Removing the ice cap of Öræfajökull central volcano, SE-Iceland: Mapping and interpretation of bedrock topography, ice volumes, subglacial troughs and implications for hazards assessments. *Jökull*, **64,** 83-84.

Mallet, J.L. 1997. Discrete modelling for natural objects. *Mathematical Geology*, **29,** 199–219.

Murray, T., Dowdeswell, J.A., Drewry, D.J. and Frearson, I. 1998. Geometric evolution and ice dynamics during a surge of Bakaninbreen, Svalbard. *Journal of Glaciology*, **44,** 263-272.

Murray, T., Stuart, G.W., Fry, M., Gamble, N.H. and Crabtree, M.D. 2000. Englacial water distribution in a temperate glacier from surface and borehole radar velocity analysis. *Journal of Glaciology*, **46,** 389–398.

Ó Cofaigh, C., Evans, D.J.A. and Smith, I.R. 2010. Large scale reorganization and sedimentation of terrestrial ice streams during a single glacial cycle. *Geological Society of America Bulletin* **122,** 743-756.

Phillips, E., Finlayson, A., Jones, L., 2013. Fracturing, block faulting, and moulin development associated with progressive collapse and retreat of a maritime glacier: Falljökull, SE Iceland. *Journal of Geophysical Research: Earth Surface,* **118,** 1-17.

Phillips, E., Finlayson, A., Bradwell, T., Everest, J. and Jones, L. 2014. Structural evolution triggers a dynamic reduction in active glacier length during rapid retreat: Evidence from Falljökull, SE Iceland. *Journal of Geophysical Research: Earth Surface*, **119,** doi:10.1002/2014JF003165.

Sensors and Software. 2003. *PulseEKKO PRO user's guide*. Sensors and Software Inc., Mississauga, Canada, 159 p.

Sharp, M. 1988. Surging glaciers – behaviour and mechanisms. *Progress in Physical Geography*, **12,** 349-370.

Sharp, M., Lawson, W. and Anderson, W. 1988. Tectonic processes in a surge type glacier. *Journal of Glaciology*, **40,** 327-340.

Sigurðsson, O. 1998. Glacier variations in Iceland 1930–1995: from the database of the Iceland Glaciological Society. *Jökull*, **45,** 3–25.

Sigurðsson, O., Jónsson, T. and Jóhannesson, T. 2007. Relation between glacier-termini variations and summer temperatures in Iceland since 1930. *Annals of Glaciology*, **46,** 170-176.

Spedding, N. and Evans, D.J.A. 2002. Sediments and landforms at Kvíárjökull, southeast Iceland: a reappraisal of the glaciated valley landsystem. *Sedimentary Geology*, **149,** 21–42.

Stokes, C.R. and Clark, C.D. 2002. Ice stream shear margin moraines. *Earth Surface Processes and Landforms* **27,** 547-558.

Stokes, C.R., Clark, C.D., Lian, O.B. and Tulaczyk, S. 2007. Ice stream sticky spots: a review of their identification and influence beneath contemporary and palaeo-ice streams. *Earth Science Reviews* **81,** 217-249.

Swift, D.A., Evans, D.J.A. and Fallick, A.E. 2006. Transverse englacial debris-rich ice bands at Kvíárjökull, southeast Iceland. *Quaternary Science Reviews*, **25,** 1708–1718.

Woodward, J., Murray, T. and McCraig, A. 2002. Formation and reorientation of structure in surge-type glacier Kongsvegen, Svalbard. *Journal of Quaternary Science*, **17,** 201-209.

Figures

Figure 1. (a) Map showing the location of the study area on the southern side of Vatnajökull in southeast Iceland; (b) Photograph of Kvíárjökull from the prominent icefall linking the glacier to its source area on Öræfajökull to the proglacial lake developed adjacent to its margin. Also shown are the large, prominent latero-frontal moraines of the Kviarmýrarkambur (southern-side of glacier) and Kambsmýrarkambur (northern-side of glacier) which enclose the glacier; (c) Photograph of the lower reaches of Kvíárjökull showing the highly crevassed/ridged “active” northern part of the glacier and the smoother, low-lying very slow moving to static southern part which is pockmarked by moulin. A large, ice-cored moraine and esker can also be seen on the surface of the glacier close to its margin; and (d) Photograph of the northern “active” margin of Kvíárjökull with a prominent ice-cliff revealing the ice core to a large moraine marking the margin of the glacier. The ice-cliff also reveals the banded nature of the glacier comprising alternating dark, relatively debris-rich and white debris-free ice.

Figure 2. Structural map of the thrusts, fractures, banding and moulin identified on the surface Kvíárjökull (see supplementary publication). Changes in the orientation of the fractures (see rose diagrams) has allowed the glacier to be divided into a number of structural domains (Domains 1 to27): (a) High resolution satellite imagery of Kvíárjökull taken in 2014 © DigitalGlobe, Inc. All Rights Reserved; and (b) detailed structural map of the glacier and rose diagrams showing the orientation (trend) of the fractures developed within the ice.

Figure 3. Enlarge section of the structural map of the upper part of Kvíárjökull (see supplementary publication): (a) High resolution satellite imagery of Kvíárjökull taken in 2014 © DigitalGlobe, Inc. All Rights Reserved; and (b) detailed structural map of the icefall.

Figure 4. Enlarge section of the structural map of the central part of Kvíárjökull (see supplementary publication): (a) High resolution satellite imagery of Kvíárjökull taken in 2014 © DigitalGlobe, Inc. All Rights Reserved; and (b) detailed structural map.

Figure 5. Enlarge section of the structural map of the lower part of Kvíárjökull (see supplementary publication): (a) High resolution satellite imagery of Kvíárjökull taken in 2014 © DigitalGlobe, Inc. All Rights Reserved; and (b) detailed structural map.

Figure 6. Detailed structural map of the thrusts, fractures and banding developed within the marginal zone of Kvíárjökull (see supplementary publication). The rose diagrams show the trend (strike) of the fractures developed within the ice and the change in their orientation helping to define the individual structural domains. Also shown are the positions of the field locations on the surface of the glacier and along its northern margin examined during the study. Insets show the location and detailed high resolution air photography obtained during the study and used to construct the structural map.

Figure 7. (a) Location of GPR profile lines (shown in red). The white outline covers much of Domain 1 and indicates the area where the glacier bed elevation has been interpolated based on the GPR data. The positions of GPR profiles 12 and 22 are shown in yellow. These profiles are shown in C and E of this figure, respectively; (b) Interpolation of glacier bed elevation for Domain 1 based GPR data; (c) GPR Profile 12 shown together with digital elevation model; (d) Detailed view of down-ice dipping reflector (interpreted as water-filled reverse fault) below the surface at the down-ice end of Profile 12. The reflector appears to offset an up-ice dipping reflector at approximately 915 m distance; and (e) GPR profile 22 form the glacier foreland, shown with interpreted structures.

Figure 8. (a) extent of the 2014 LiDAR and UAV-derived DEM (gold) overlain on the Veðurstofa Íslands DEM from 2010 (grey hillshade). White boundary line indicates intersection of both surfaces; and (b) 2014 LiDAR and UAV- derived DEM, coloured by height variation above and below the 2010 surface. Change in elevation varies from circa +43 m to -8.5 m. Comparison of the two surfaces shows the active northeast margin has advanced c. 220 m from 2010 to 2014, clearly indicated by displacement of the controlled moraine, and advance of the active margin into the proglacial lake. The stationary/ slow-moving ice (Domain 1) has lowered by a maximum of 8.5 m in the central south-eastern area.

Figure 9. (a) Recent push-moraines developed along the northern margin of Kvíárjökull; (b) Photograph of the northern lateral margin of Kvíárjökull showing the banded nature of the ice, the presence of a prominent fault zone close to the margin and an ice-marginal meltwater channel feeding into the ice-marginal lake; and (c) Photograph showing the marked changes in the angle of dip of the banding within the ice as a result of faulting.

Figure 10. (a) Structural domains map showing the architecture of Kvíárjökull and, in particular, the presence of a corridor of elongate to lobate domains along the axis of the glacier which widens toward the northern margin of the glacier. Purple and blue colours indicate the more active parts of the glacier, and the green coloured domains representing the slower moving or static marginal zones (see text for details); (b) Cartoon showing the relationship between the various types of Riedel shears developed on the southern side of Kvíárjökull and the overall ice movement direction; and (c) Detailed interpretation of the structure of the central and northern parts of the marginal zone of Kvíárjökull with the arcuate pattern of fractures defining a dextral brittle shear zone.

Figure 11. (a) to (c) Up-ice dipping thrusts and rare folds deforming the banding developed within Kvíárjökull.

Figure 12. Extracts from the high resolution 2014 satellite imagery of Kvíárjökull (© DigitalGlobe, Inc. All Rights Reserved) showing the presence of large-scale sinistral (a) and dextral (b) brittle shear zones deforming the glacier defined by the presence of well-developed, open, en-echelon tension fissures.

Figure 13. (a) to (c) Laterally extensive, steeply inclined to subvertical fractures orientated parallel to the axis of the glacier. These fractures are exposed close to, and within the boundary zone separating the slow moving to static low-lying part of the Kvíárjökull and the highly crevassed, active northern part of the glacier. These ice-flow parallel fractures include normal and reverse faults which off-set (displacement 10 to 30 cm) the glacier surface with a consistent downthrow toward the north.

Figure 14. (a) Down-ice dipping reverse (compressional) faults defining the margin of an apparently “up-thrown” block developed close to the margin of Kvíárjökull; and (b) Schematic cross-section showing the interpretation of these structures.

Figure 15. (a) to (d) Well-developed, arcuate to sigmoidal shaped, en-echelon, open tension fissures developed between laterally extensive fractures recording a consistent dextral sense of shear; and (e) Asymmetrical S-C-like fabric marking a narrow zone of brittle-ductile shear developed along a laterally extensive fracture orientated parallel to the axis of the glacier. Note the fine-grained, sugary looking nature of the ice within this shear zone and dextral sense of shear recorded by the foliation.

Figure 16. Aerial photographs, fracture maps and structural domains maps showing the structural evolution of the lower reaches of Kvíárjökull between 1945 and 2003. (a) 1945; (b) 1964; (c) 1980; (d) 1998; and (e) 2003 (see text for details).

Tables

Table 1. Summary of the key structural components within the domains (1 to 27) identified within the different parts of Kvíárjökull.

Location within Kvíárjökull	Structural Domains (1 to 27)	Dominant Structures	Interpretation
Ice fall	16, 17, 18	Elongate structural domains characterised by arcuate to irregular (folded), transverse, convex down-ice, open crevasses and normal faults	Active part of glacier feeding ice to its lower reaches. The domains represent individual flow units with the crevasses and faults forming due to gravitational failure and rotational-slip
Southern lateral margin	1, 21, 22, 26	Domains 21, 22 and 26 highly elongate structural domains dominated by straight to curved to hook-like, convex down-ice fractures orientated oblique to the glacier margin. These earlier fractures are deformed by ENE-WSW-trending dextral (right lateral) shear zones marked by en-echelon tension fissures. Domain 1 is structurally more complex comprising radiating convex down-ice fractures, longitudinal flow-parallel fractures and up-ice dipping thrusts	Inactive part of glacier composed of stationary or very slow moving ice. Curved, hook-like fractures developed in response to a combination of lateral shear stresses and longitudinal compression into earlier forward motion of Kvíárjökull. Domain 1 presents an area of stationary/very slow moving ice adjacent to the SE-side of the snout. Radiating fractures and thrusts within this domain interpreted in terms of deformation occurring towards the snout of the glacier in response to earlier plug-like flow
Northern lateral margin	9, 10, 11	Elongate structural domains characterised by NE-SW-trending fractures oblique to the axis of Kvíárjökull. These earlier fractures are deformed by ENE-WSW-trending sinistral (left lateral) shear zones marked by en-echelon tension fissures	Inactive part of glacier composed of stationary or very slow moving ice. Oblique fractures interpreted as chevron crevasses developed in response to the combination of lateral shear stress imposed during earlier forward motion of Kvíárjökull in response to plug-like flow
Central zone: lobes	19, 20, 23, 24, 25, 27	Elongate, topographically higher lobes of ice within the central zone are and composed of highly crevassed ice. Domains higher in the glacier comprise a set of arcuate, convex down-ice fractures. Domain 27 represents the largest lobe and comprises a set of radiating, fan-like crevasses cross-cut by a set of short open fractures. Earlier formed fractures are deformed by ENE-WSW-trending dextral (right lateral) shear zones marked	Active part of glacier with the elongate lobes of ice being interpreted as individual flow units that move independently or "pulse". The size of the lobes increases down-ice indicating that the size (volume) of these pulses of ice changes over time or that they can incorporate/entrain ice from older flow units and/or the margin of the glacier as they move down-ice. Radiating fracture pattern within Domain 27 interpreted in terms of deformation caused by longitudinal compression and lateral extension as the flow unit overrides the static/slow moving ice located on the SE-side of the snout. Narrow shear zones deforming the earlier formed fracture sets may result from either shearing imposed by the passage of later pulses of ice, or the partitioning of deformation into increasingly narrower zones

		by en-echelon tension fissures	as the ice begins to stop moving and the flow unit "locks up". The lobes are cross cut by the elongate, laterally continuous axial zone which forms the main conduit for transmitting ice from the icefall to the NE-margin of the Kvíárjökull. The variation from open to closed transverse fractures reflects changes in the flow regime down the axis of the glacier resulted from the switching between localised extension (open) and compression (closed).
Central zone: axial zone	6, 7, 12, 13, 14, 15	Elongate domains forming a highly crevassed, laterally continuous, relatively narrow zone along the axis of the glacier. They comprise a set of longitudinal (flow-parallel) crevasses crosscut by a set of arcuate (convex down-ice), open to closed fractures developed transverse to flow. Transverse fractures are locally deformed by ENE-WSW-trending dextral (right lateral) shear zones marked by en-echelon tension fissures	
Northeast frontal margin - subzone (i)	7, 8	Relatively poorly exposed, largely debris covered northern subzone developed adjacent to the NE-margin. The orientation of the dominant ice-flow parallel fractures ranges from ENE-WSW to NE-SW	Active part of the glacier which accommodated a minor readvance in 2013-14 leading to the formation of an ice-cored push-moraine along the NE-margin of Kvíárjökull. The crevasse pattern within the ice indicates that flow is deflected towards the NE-side of the glacier, probably due to the presence of essentially static ice (Domain 1) on the SE-side of the snout. The boundary between the highly crevassed active part of the glacier and the relatively smooth slow moving to static ice is marked by a wide, structurally complex, dextral (right-lateral) shear zone and zone of closely spaced longitudinal fractures and dextral strike-slip faults. The shear zone and strike-slip faults help ice within the active NE-part of the glacier move past the static ice located to the south
Northeast frontal margin - subzone (ii)	2, 3, 4, 5	Structurally complex subzone comprising a series of arcuate, S-shaped domains characterised by well-developed, closely spaced curved, open to closed, steeply inclined fractures. Asymmetrical shape of fractures records an E/ESE directed (dextral) sense of shear. The boundary between the dextral shear zone and Domain 1 to the south is gradational over several tens of metres, with the dextral strike-slip displacement being taken up by laterally extensive flow-parallel fractures.	

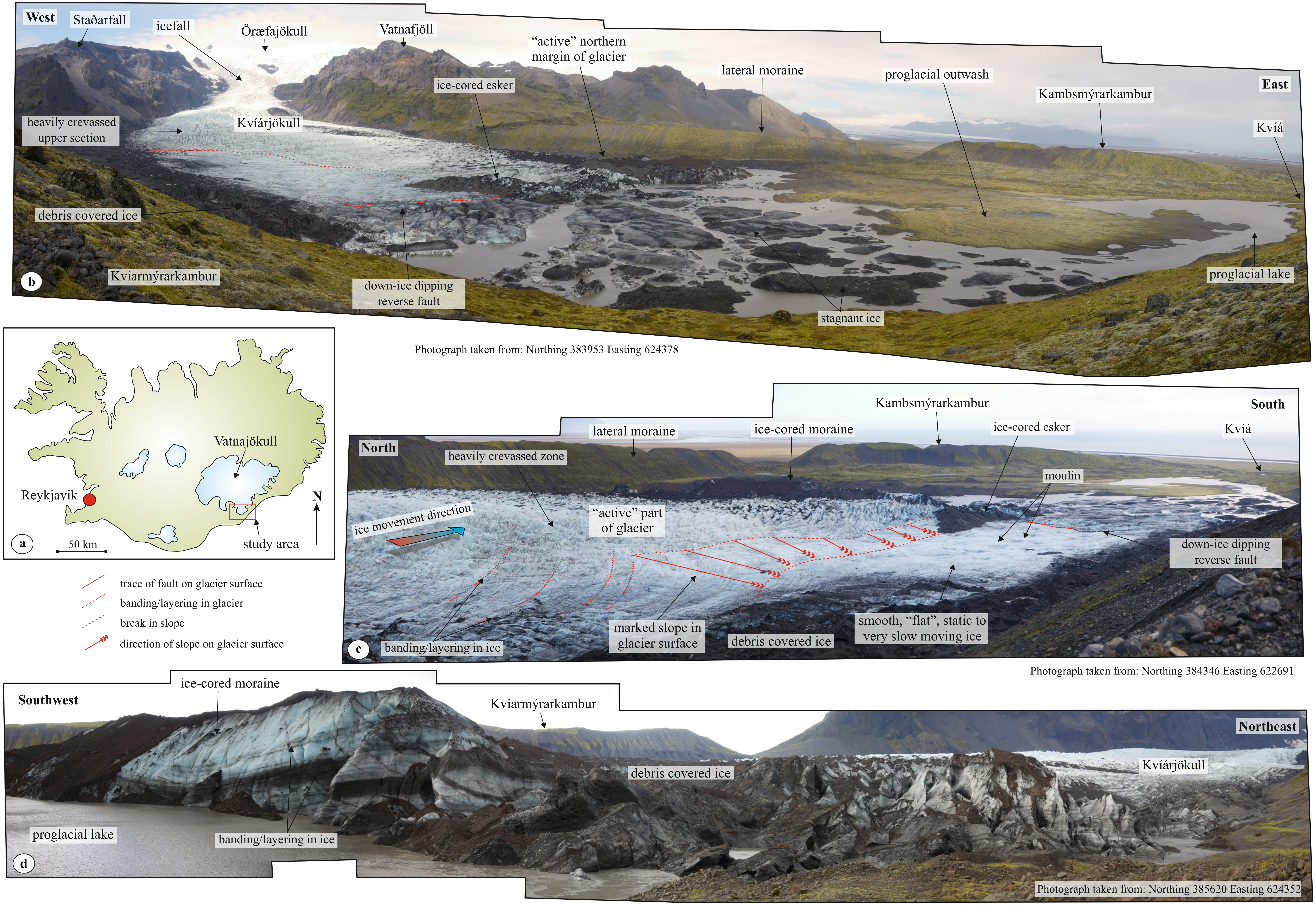

West
Staðarfall
icefall
Öræfajökull
Vatnafjöll
"active" northern margin of glacier
ice-cored esker
lateral moraine
proglacial outwash
Kambsmýrarkambur
East
Kvíá
heavily crevassed upper section
Kvíárjökull
debris covered ice
Kviarmýrarkambur
down-ice dipping reverse fault
stagnant ice
proglacial lake
b
Photograph taken from: Northing 383953 Easting 624378
Vatnajökull
Reykjavik
N
a
50 km
study area
trace of fault on glacier surface
banding/layering in glacier
break in slope
direction of slope on glacier surface
North
lateral moraine
ice-cored moraine
Kambsmýrarkambur
South
ice-cored esker
Kvíá
heavily crevassed zone
moulin
ice movement direction
"active" part of glacier
down-ice dipping reverse fault
marked slope in glacier surface
debris covered ice
smooth, "flat", static to very slow moving ice
banding/layering in ice
c
Photograph taken from: Northing 384346 Easting 622691
Southwest
ice-cored moraine
Kviarmýrarkambur
Northeast
debris covered ice
Kvíárjökull
proglacial lake
banding/layering in ice
d
Photograph taken from: Northing 385620 Easting 624352

b
Domains 1 to 27 - structural domains (see text for details)
limited of mapped area of the glacier
coloured lines, linear features identified on glacier surface including closed and open fractures, banding...etc
500 m
N
Domain 17 (N = 1246)
Domain 16 (N = 1217)
Domain 18 (N = 1178)
Domain 15 (N = 356)
Domain 19 (N = 918)
Domain 14 (N = 250)
Domain 13 (N = 370)
Domain 12 (N = 368)
Domain 11 (N = 3145)
Domain 20 (N = 531)
Domain 21 (N = 939)
Domain 6 (N = 1866)
Domain 9 (N = 1043)
Domain 10 (N = 448)
Domain 5 (N = 243)
Domain 7 (N = 1037)
Domain 8 (N = 240)
Domain 22 (N = 202)
Domain 23 (N = 258)
Domain 24 (N = 588)
Domain 26 (N = 1379)
Domain 25 (N = 1060)
Domain 27 (N = 2091)
Domain 27 cross-cutting features (N = 866)
Domain 1 (N = 845)
fractures and reverse faults near margin of glacier (N = 117)
Domain 2 (N = 314)
Domain 3 (N = 210)
Domain 4 (N = 229)
prominent bedrock outcrop
prominent bedrock outcrop
Domain 1
Domain 2
Domain 3
Domain 4
Domain 5
Domain 6
Domain 7
Domain 8
Domain 9
Domain 10
Domain 11
Domain 12
Domain 13
Domain 14
Domain 15
Domain 16
Domain 17
Domain 18
Domain 19
Domain 20
Domain 21
Domain 22
Domain 23
Domain 24
Domain 25
Domain 26
Domain 27
a
Öræfajökull
Vatnafjöll
debris covered ice
Kviárjökull
Staðarfall
Kambsmýrarkambur
extent of air photography taken using Phantom quadcopter
Kviár
proglacial lake
Kviarmýrarkambur
500 m

b
Domains 1 to 27 - structural domains (see text for details)
limited of mapped area of the glacier
coloured lines, linear features identified on glacier surface including closed and open fractures, banding...etc
N
500 m
Domain 1 (N = 845)
Domain 2 (N = 314)
Domain 3 (N = 210)
Domain 4 (N = 229)
Domain 5 (N = 243)
Domain 6 (N = 1866)
Domain 7 (N = 1037)
Domain 8 (N = 240)
Domain 9 (N = 1043)
Domain 10 (N = 448)
Domain 11 (N = 3145)
Domain 12 (N = 368)
Domain 13 (N = 370)
Domain 14 (N = 250)
Domain 15 (N = 356)
Domain 16 (N = 1217)
Domain 17 (N = 1246)
Domain 18 (N = 1178)
Domain 19 (N = 918)
Domain 20 (N = 531)
Domain 21 (N = 939)
Domain 22 (N = 202)
Domain 23 (N = 258)
Domain 24 (N = 588)
Domain 25 (N = 1060)
Domain 26 (N = 1379)
Domain 27 (N = 2091)
Domain 27 cross-cutting features (N = 866)
fractures and reverse faults near margin of glacier (N = 117)
prominent bedrock outcrop
prominent bedrock outcrop
a
Öræfajökull
Vatnafjöll
debris covered ice
Kviárjökull
Staðarfall
Kambsmýrarkambur
extent of air photography taken using Phantom quadcopter
Kviá
proglacial lake
Kviarmýrarkambur
500 m
N

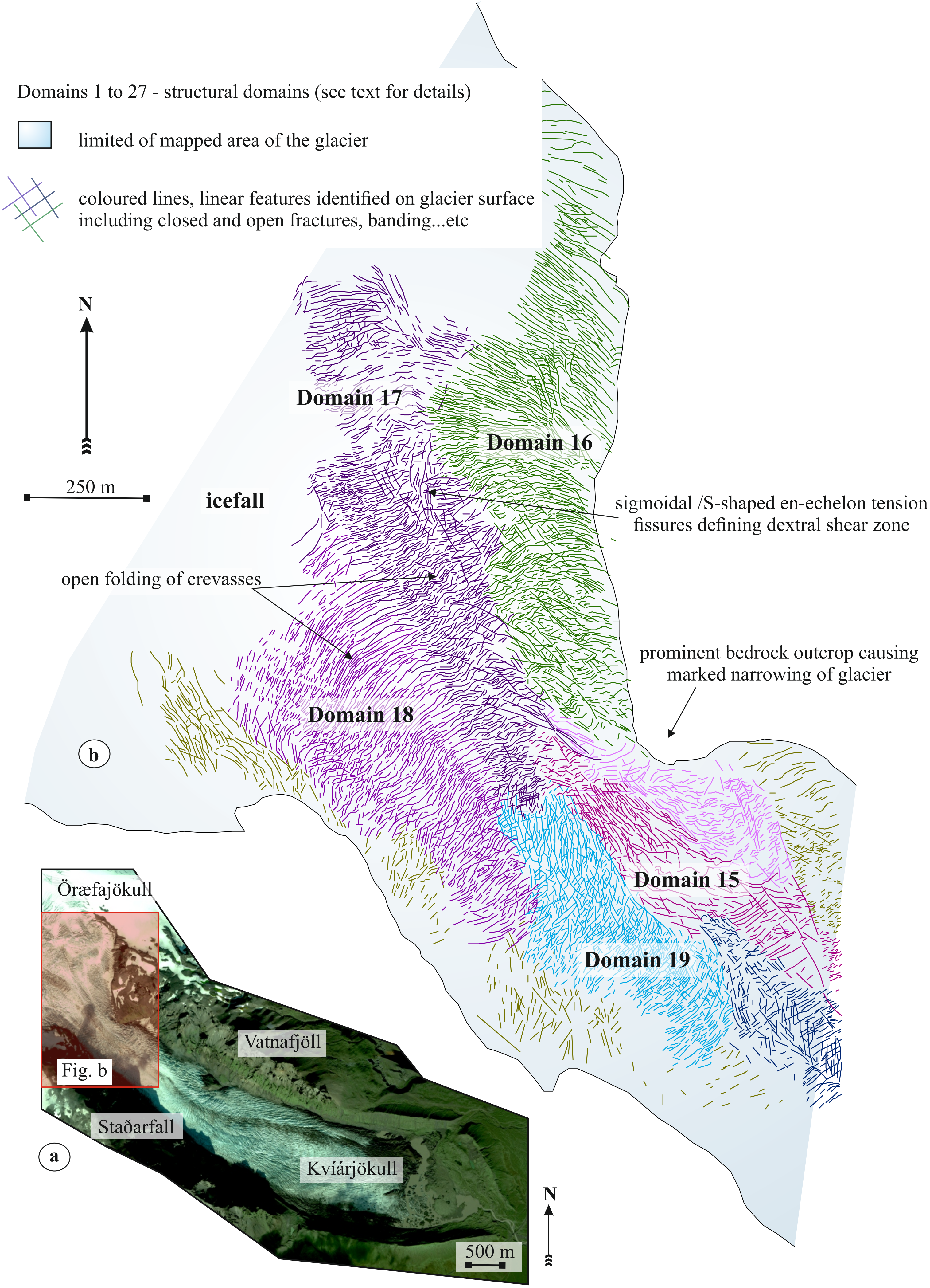
Domains 1 to 27 - structural domains (see text for details)
limited of mapped area of the glacier
coloured lines, linear features identified on glacier surface including closed and open fractures, banding...etc
N
250 m
icefall
Domain 17
Domain 16
Domain 18
Domain 15
Domain 19
sigmoidal /S-shaped en-echelon tension fissures defining dextral shear zone
open folding of crevasses
prominent bedrock outcrop causing marked narrowing of glacier
b
Öræfajökull
Fig. b
Vatnafjöll
Staðarfall
Kvíárjökull
a
N
500 m

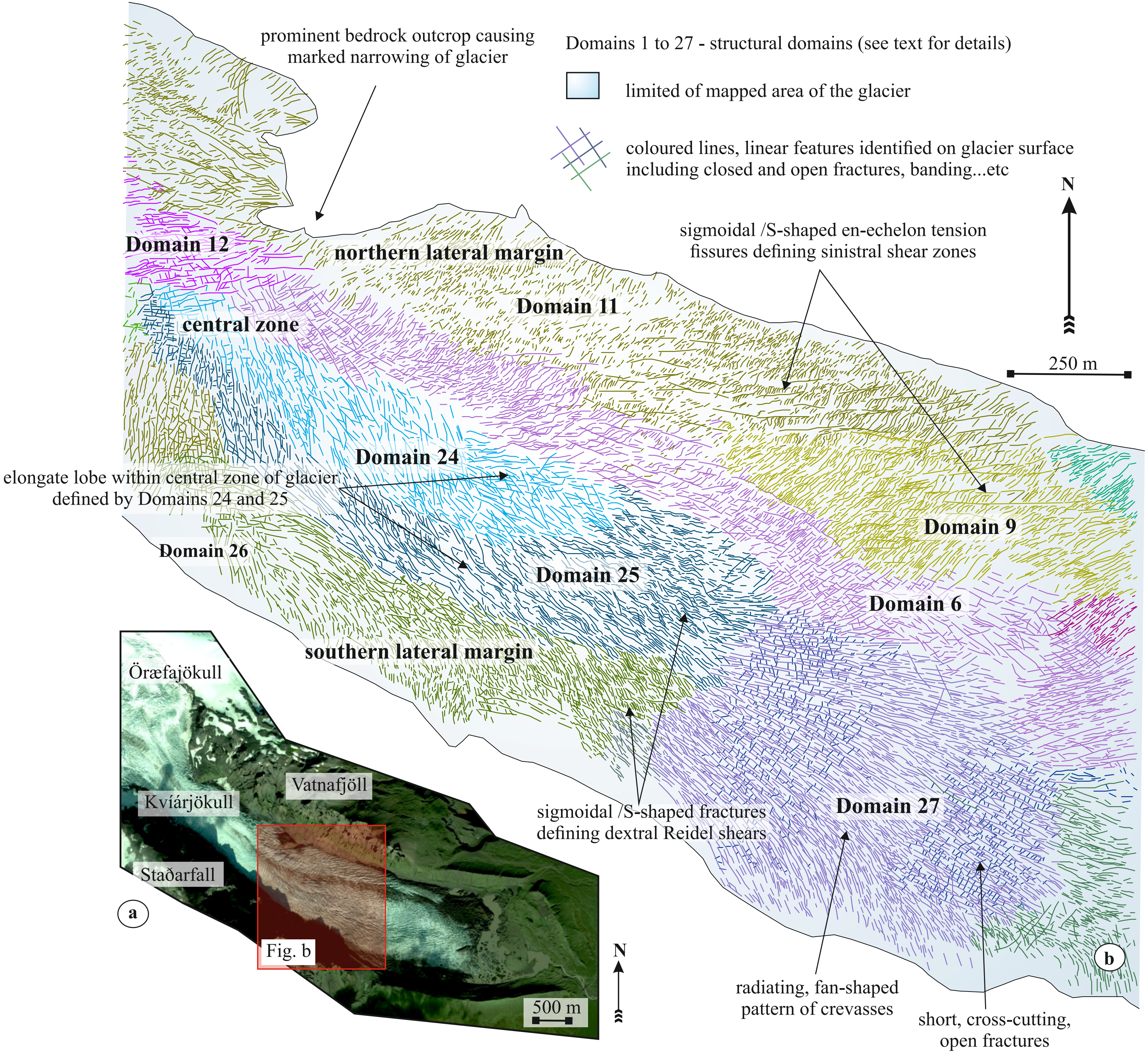
prominent bedrock outcrop causing marked narrowing of glacier
Domains 1 to 27 - structural domains (see text for details)
limited of mapped area of the glacier
coloured lines, linear features identified on glacier surface including closed and open fractures, banding...etc
N
250 m
sigmoidal /S-shaped en-echelon tension fissures defining sinistral shear zones
Domain 12
northern lateral margin
Domain 11
central zone
Domain 24
elongate lobe within central zone of glacier defined by Domains 24 and 25
Domain 9
Domain 26
Domain 25
Domain 6
southern lateral margin
Öræfajökull
Vatnafjöll
Kvíárjökull
Staðarfall
a
Fig. b
N
500 m
sigmoidal /S-shaped fractures defining dextral Reidel shears
Domain 27
radiating, fan-shaped pattern of crevasses
short, cross-cutting, open fractures
b

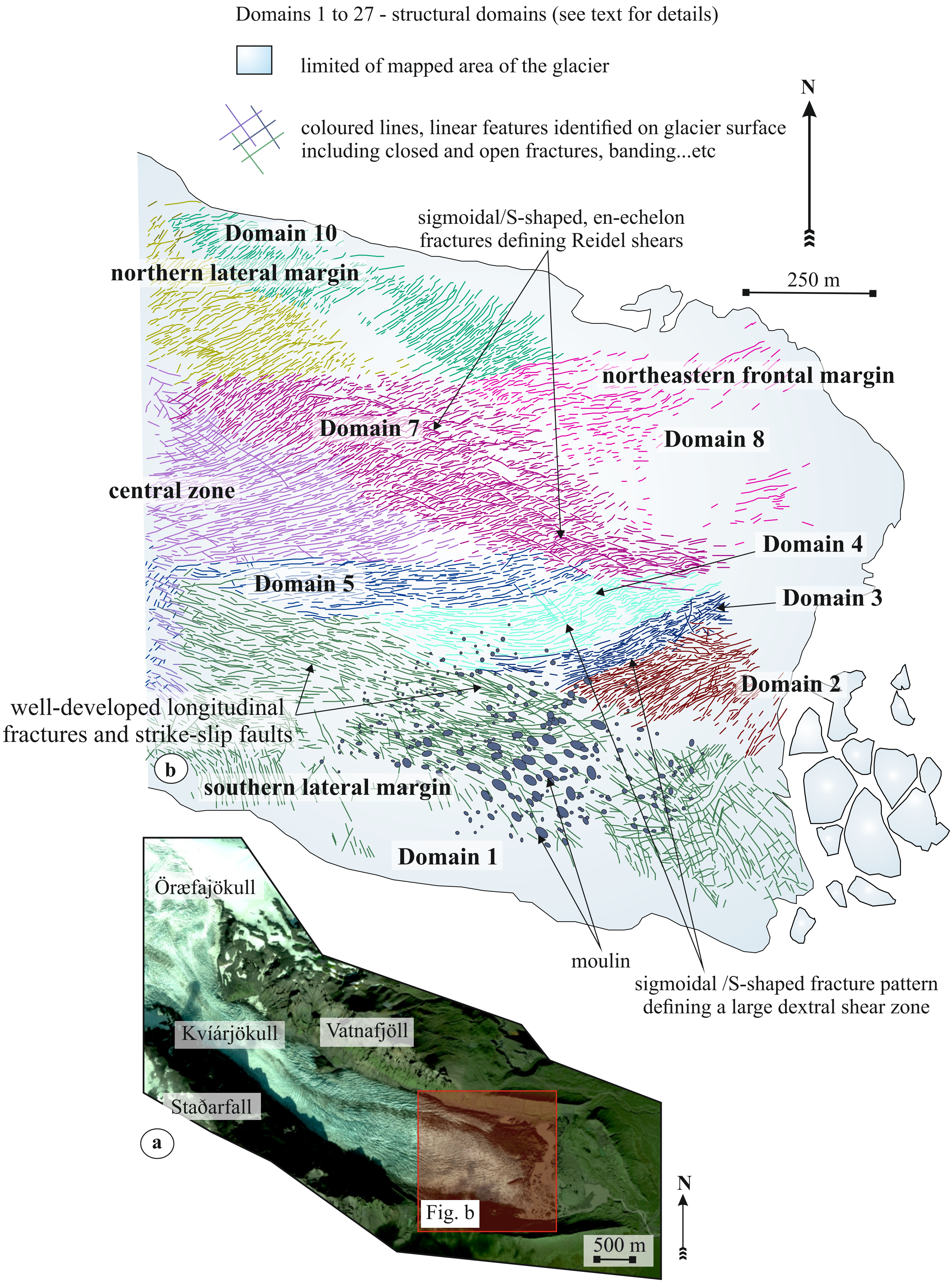
Domains 1 to 27 - structural domains (see text for details)
limited of mapped area of the glacier
coloured lines, linear features identified on glacier surface including closed and open fractures, banding...etc
N
250 m
sigmoidal/S-shaped, en-echelon fractures defining Reidel shears
Domain 10
northern lateral margin
northeastern frontal margin
Domain 7
Domain 8
central zone
Domain 4
Domain 5
Domain 3
Domain 2
well-developed longitudinal fractures and strike-slip faults
b
southern lateral margin
Domain 1
moulin
sigmoidal /S-shaped fracture pattern defining a large dextral shear zone
Öræfajökull
Kvíárjökull
Vatnafjöll
Staðarfall
a
Fig. b
N
500 m

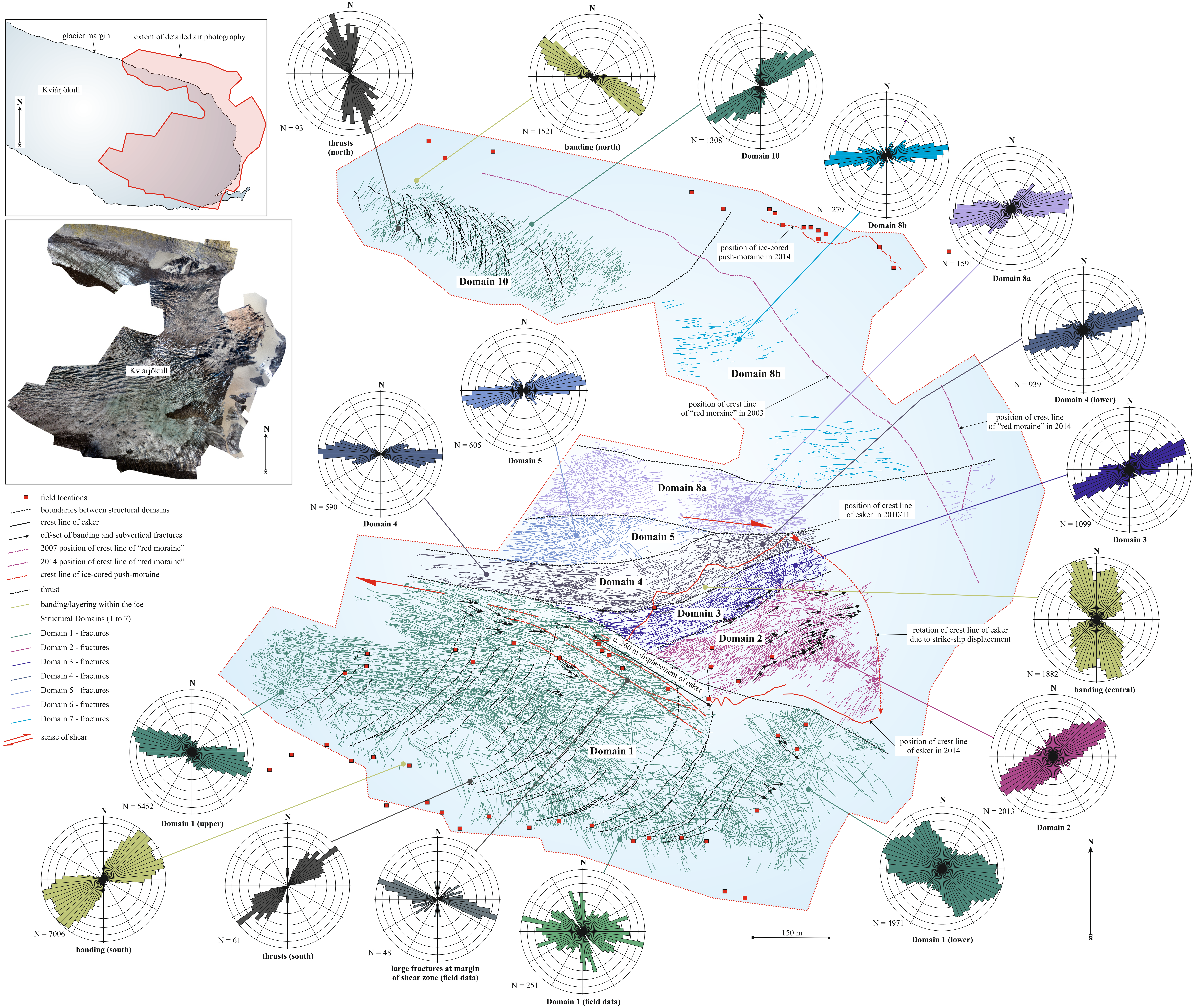

glacier margin
extent of detailed air photography
Kviárjökull
N
Kviárjökull
N
field locations
boundaries between structural domains
crest line of esker
off-set of banding and subvertical fractures
2007 position of crest line of "red moraine"
2014 position of crest line of "red moraine"
crest line of ice-cored push-moraine
thrust
banding/layering within the ice
Structural Domains (1 to 7)
Domain 1 - fractures
Domain 2 - fractures
Domain 3 - fractures
Domain 4 - fractures
Domain 5 - fractures
Domain 6 - fractures
Domain 7 - fractures
sense of shear
N = 93
thrusts (north)
N = 1521
banding (north)
N = 1308
Domain 10
N = 279
Domain 8b
N = 1591
Domain 8a
N = 939
Domain 4 (lower)
N = 1099
Domain 3
N = 1882
banding (central)
N = 2013
Domain 2
N = 4971
Domain 1 (lower)
N = 251
Domain 1 (field data)
N = 48
large fractures at margin of shear zone (field data)
N = 61
thrusts (south)
N = 7006
banding (south)
N = 5452
Domain 1 (upper)
N = 590
Domain 4
N = 605
Domain 5
Domain 10
Domain 8b
Domain 8a
Domain 5
Domain 4
Domain 3
Domain 2
Domain 1
position of ice-cored push-moraine in 2014
position of crest line of "red moraine" in 2003
position of crest line of "red moraine" in 2014
position of crest line of esker in 2010/11
rotation of crest line of esker due to strike-slip displacement
position of crest line of esker in 2014
c. 260 m displacement of esker
150 m
N

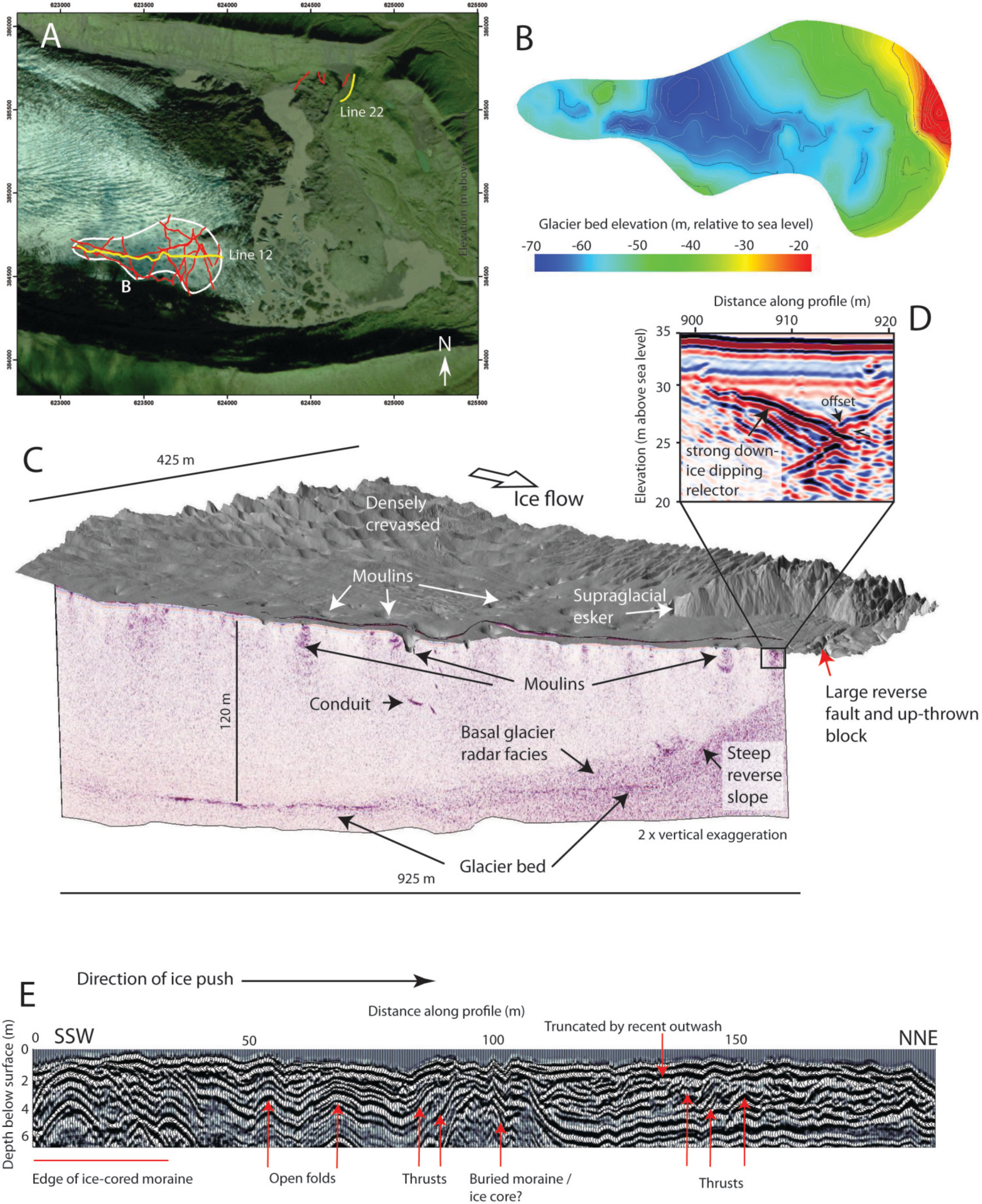

A
623000
623500
624000
624500
625000
625500
386000
385500
385000
384500
384000
Line 22
Line 12
B
N
B
Glacier bed elevation (m, relative to sea level)
-70
-60
-50
-40
-30
-20
C
425 m
Ice flow
Densely crevassed
Moulins
Supraglacial esker
Moulins
Conduit
120 m
Basal glacier radar facies
Steep reverse slope
Glacier bed
Large reverse fault and up-thrown block
2 x vertical exaggeration
925 m
D
Distance along profile (m)
900
910
920
Elevation (m above sea level)
35
30
25
20
offset
strong down-ice dipping relector
E
Direction of ice push
Distance along profile (m)
SSW
NNE
0
50
100
150
Depth below surface (m)
0
2
4
6
Truncated by recent outwash
Edge of ice-cored moraine
Open folds
Thrusts
Buried moraine / ice core?
Thrusts

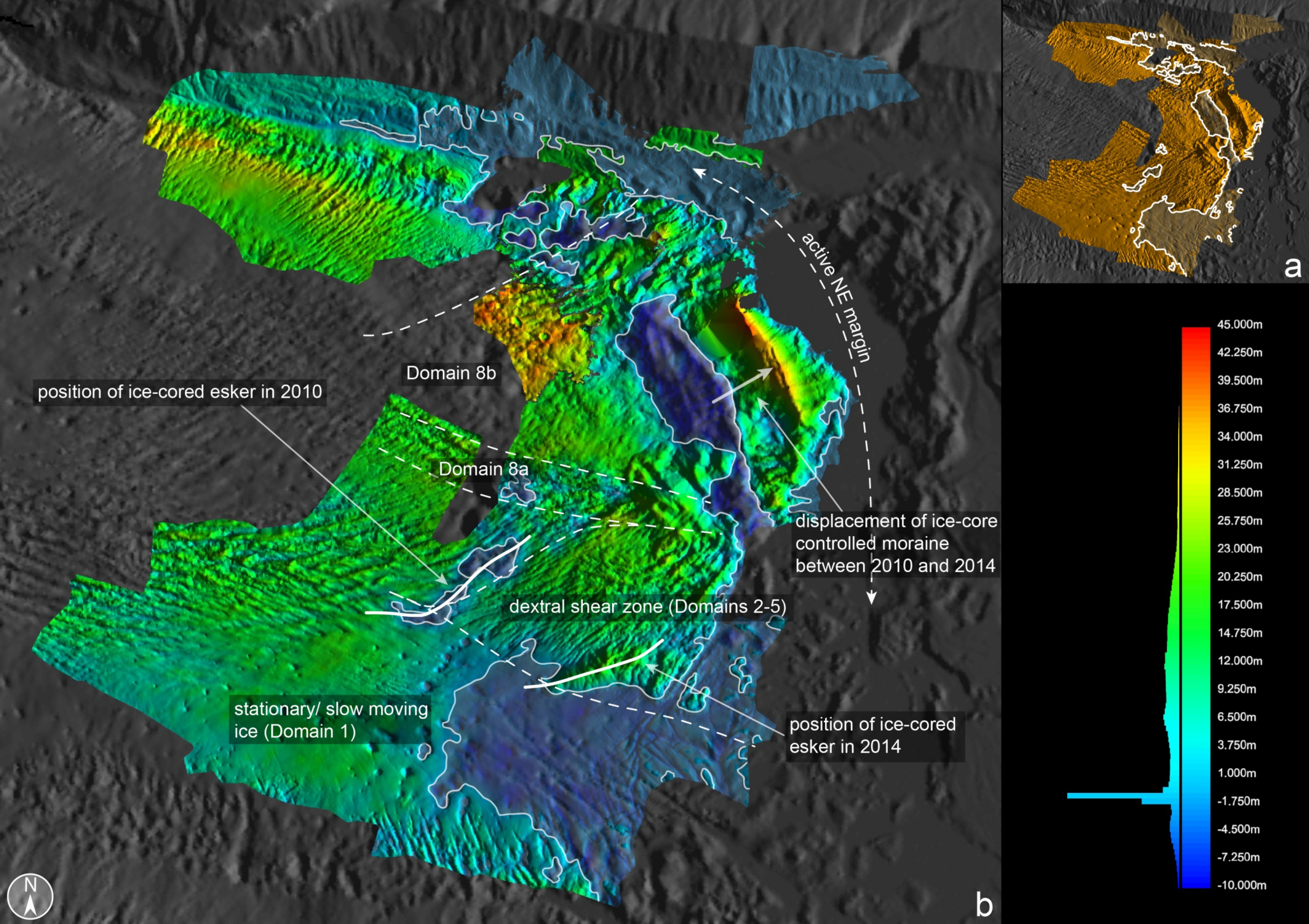

active NE margin
Domain 8b
position of ice-cored esker in 2010
Domain 8a
displacement of ice-core controlled moraine between 2010 and 2014
dextral shear zone (Domains 2-5)
stationary/ slow moving ice (Domain 1)
position of ice-cored esker in 2014
N
b
a
45.000m
42.250m
39.500m
36.750m
34.000m
31.250m
28.500m
25.750m
23.000m
20.250m
17.500m
14.750m
12.000m
9.250m
6.500m
3.750m
1.000m
-1.750m
-4.500m
-7.250m
-10.000m

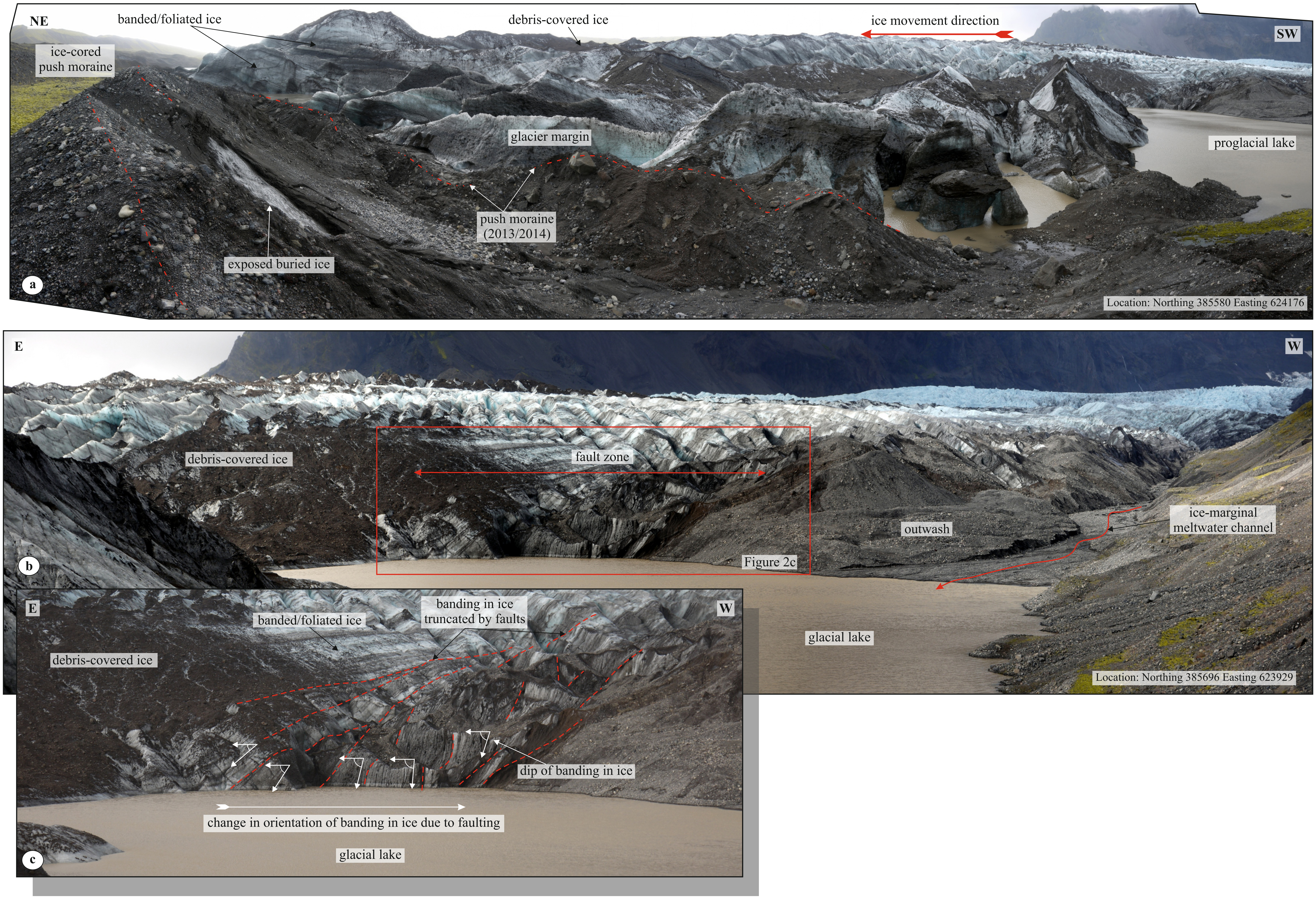

NE
banded/foliated ice
debris-covered ice
ice movement direction
SW
ice-cored push moraine
glacier margin
proglacial lake
push moraine (2013/2014)
exposed buried ice
a
Location: Northing 385580 Easting 624176
E
W
debris-covered ice
fault zone
outwash
ice-marginal meltwater channel
b
Figure 2c
glacial lake
Location: Northing 385696 Easting 623929
E
banded/foliated ice
banding in ice truncated by faults
W
debris-covered ice
dip of banding in ice
change in orientation of banding in ice due to faulting
glacial lake
c

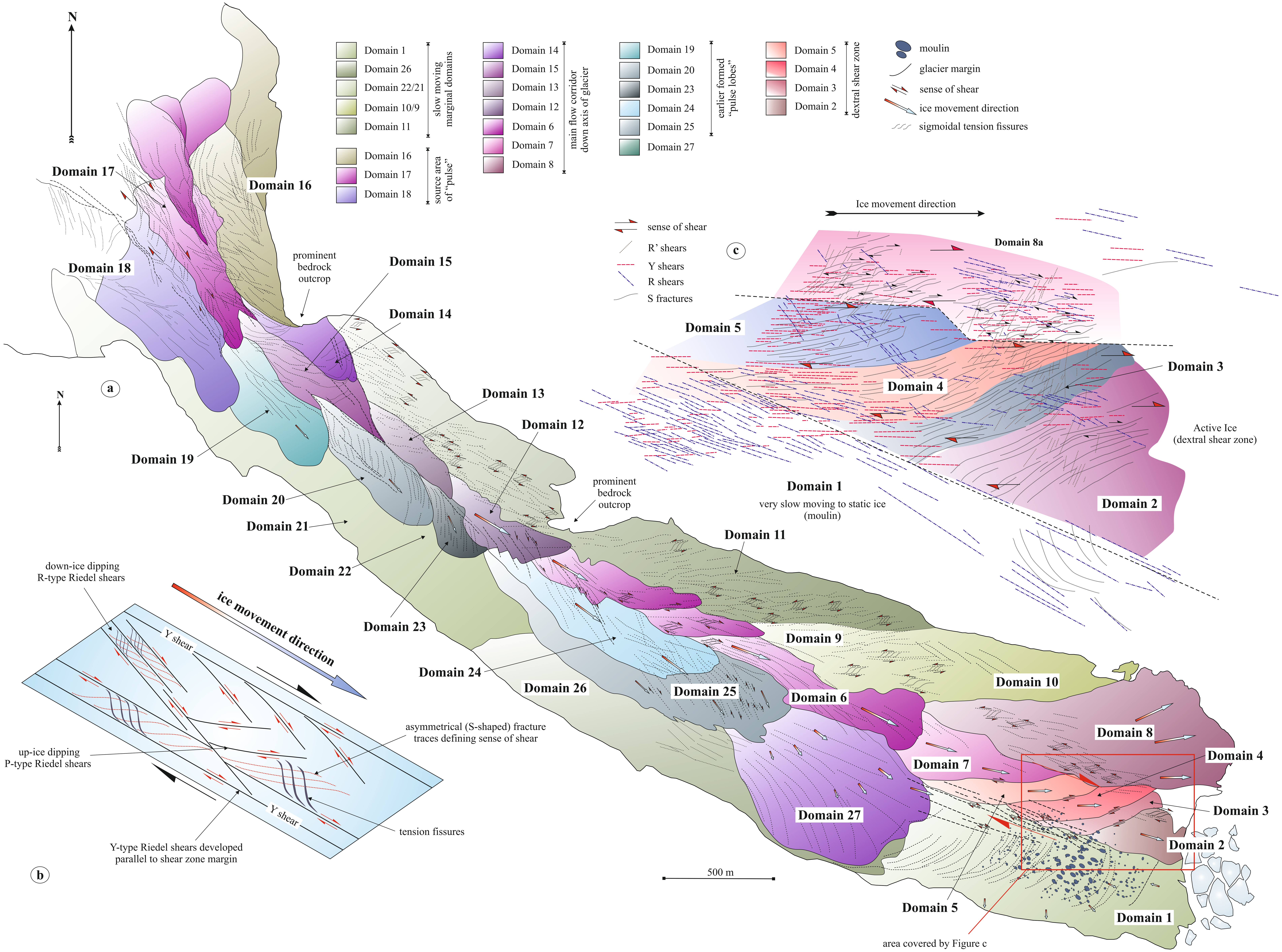

N
Domain 1
Domain 26
Domain 22/21
Domain 10/9
Domain 11
slow moving marginal domains
Domain 16
Domain 17
Domain 18
source area of "pulse"
Domain 14
Domain 15
Domain 13
Domain 12
Domain 6
Domain 7
Domain 8
main flow corridor down axis of glacier
Domain 19
Domain 20
Domain 23
Domain 24
Domain 25
Domain 27
earlier formed "pulse lobes"
Domain 5
Domain 4
Domain 3
Domain 2
dextral shear zone
moulin
glacier margin
sense of shear
ice movement direction
sigmoidal tension fissures
a
prominent bedrock outcrop
Domain 9
Domain 10
500 m
area covered by Figure c
b
down-ice dipping R-type Riedel shears
Y shear
ice movement direction
up-ice dipping P-type Riedel shears
asymmetrical (S-shaped) fracture traces defining sense of shear
tension fissures
Y-type Riedel shears developed parallel to shear zone margin
c
Ice movement direction
R' shears
Y shears
R shears
S fractures
Domain 8a
Active Ice
(dextral shear zone)
very slow moving to static ice
(moulin)

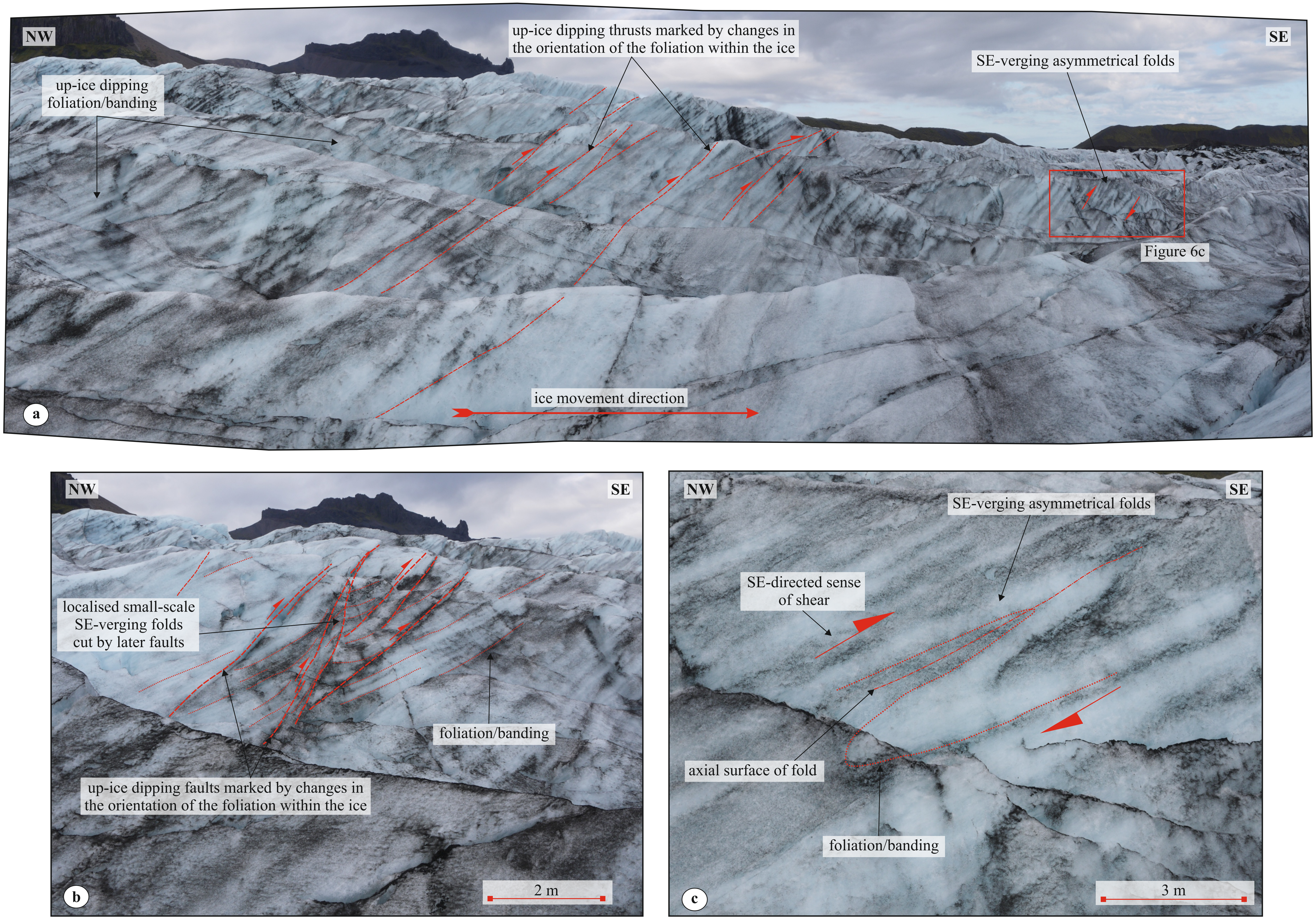
NW
SE
up-ice dipping thrusts marked by changes in the orientation of the foliation within the ice
SE-verging asymmetrical folds
up-ice dipping foliation/banding
Figure 6c
ice movement direction
a
NW
SE
localised small-scale SE-verging folds cut by later faults
foliation/banding
up-ice dipping faults marked by changes in the orientation of the foliation within the ice
2 m
b
NW
SE
SE-verging asymmetrical folds
SE-directed sense of shear
axial surface of fold
foliation/banding
3 m
c

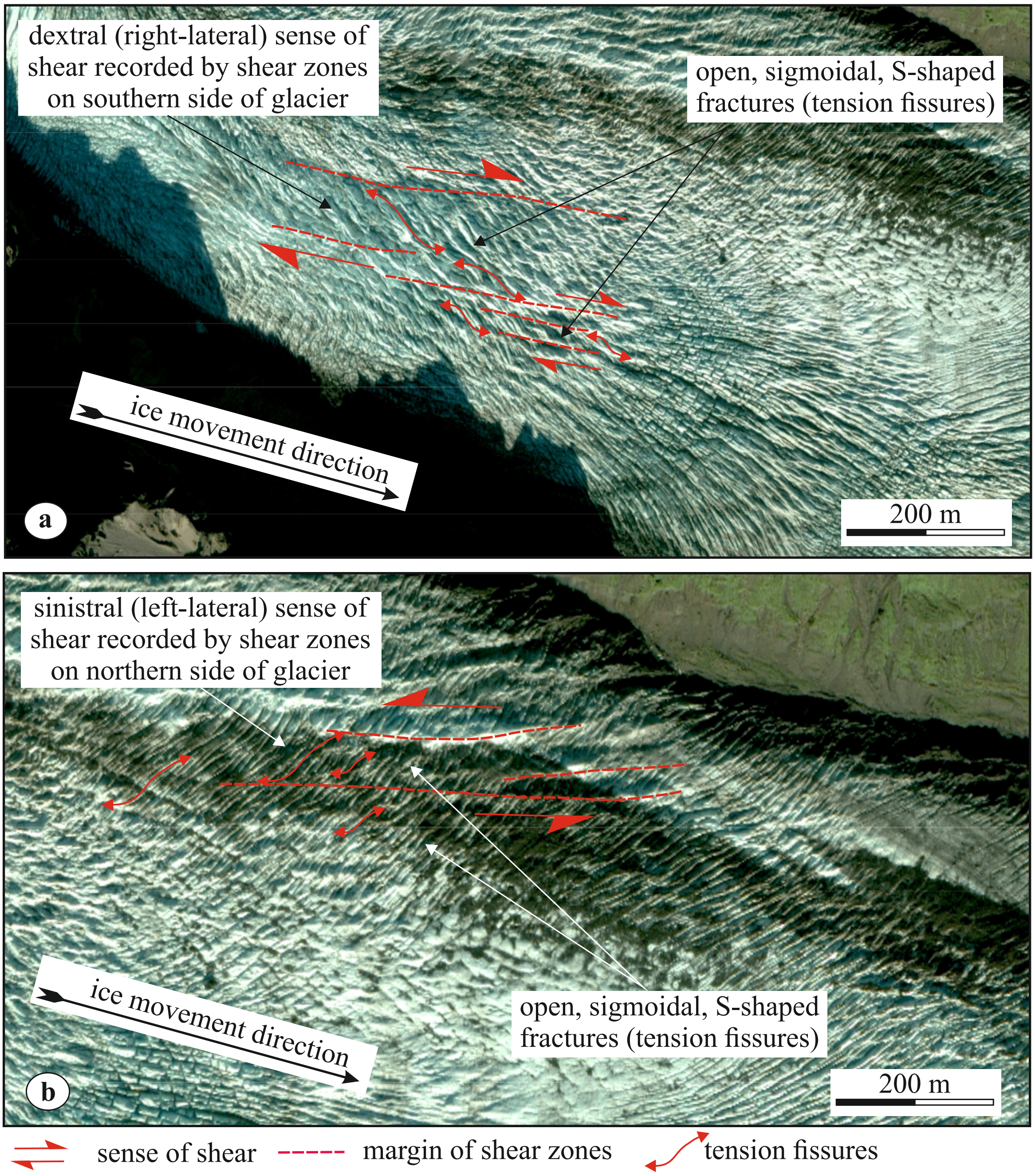
dextral (right-lateral) sense of shear recorded by shear zones on southern side of glacier
open, sigmoidal, S-shaped fractures (tension fissures)
ice movement direction
200 m
a
sinistral (left-lateral) sense of shear recorded by shear zones on northern side of glacier
open, sigmoidal, S-shaped fractures (tension fissures)
ice movement direction
200 m
b
sense of shear
margin of shear zones
tension fissures

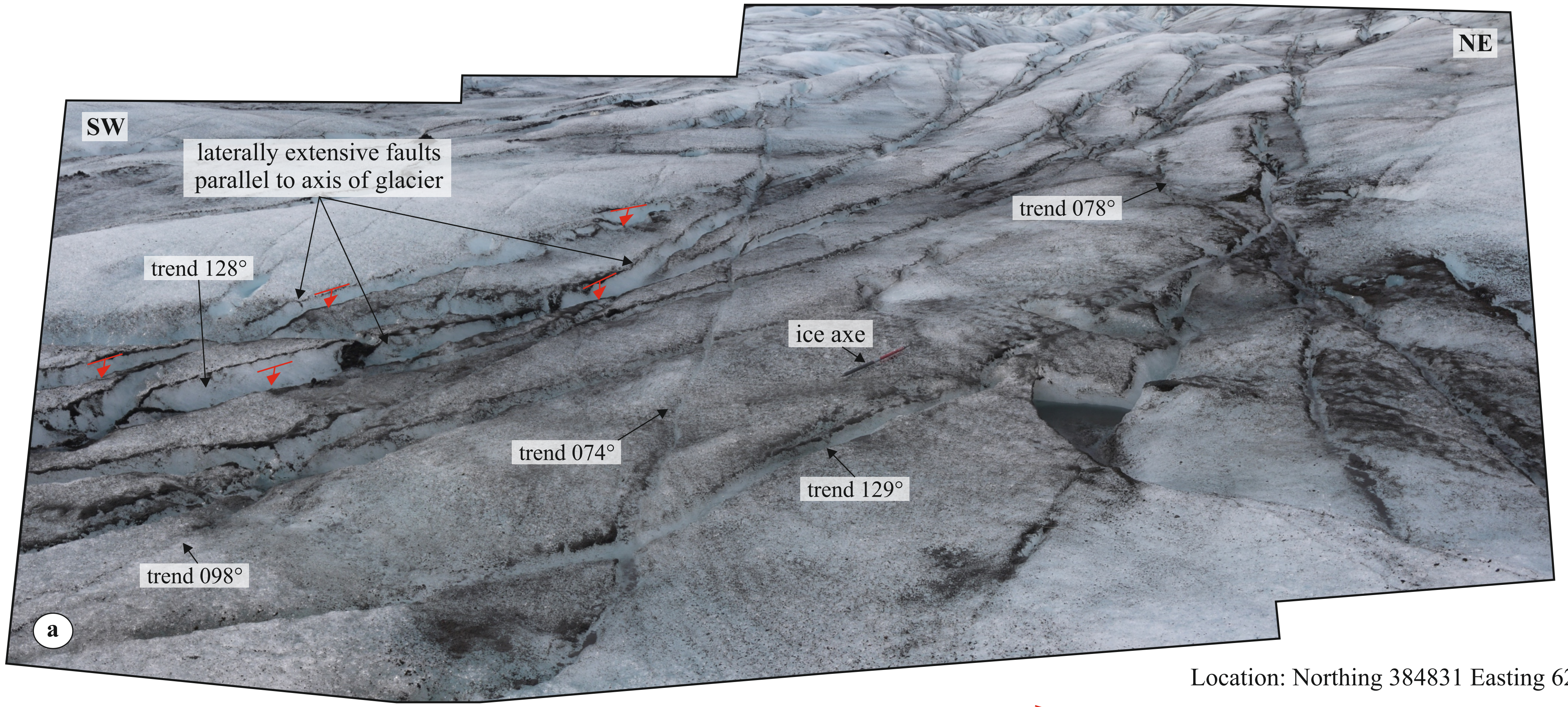

Location: Northing 384831 Easting 623589

orientation and dip direction of exposed fault planes

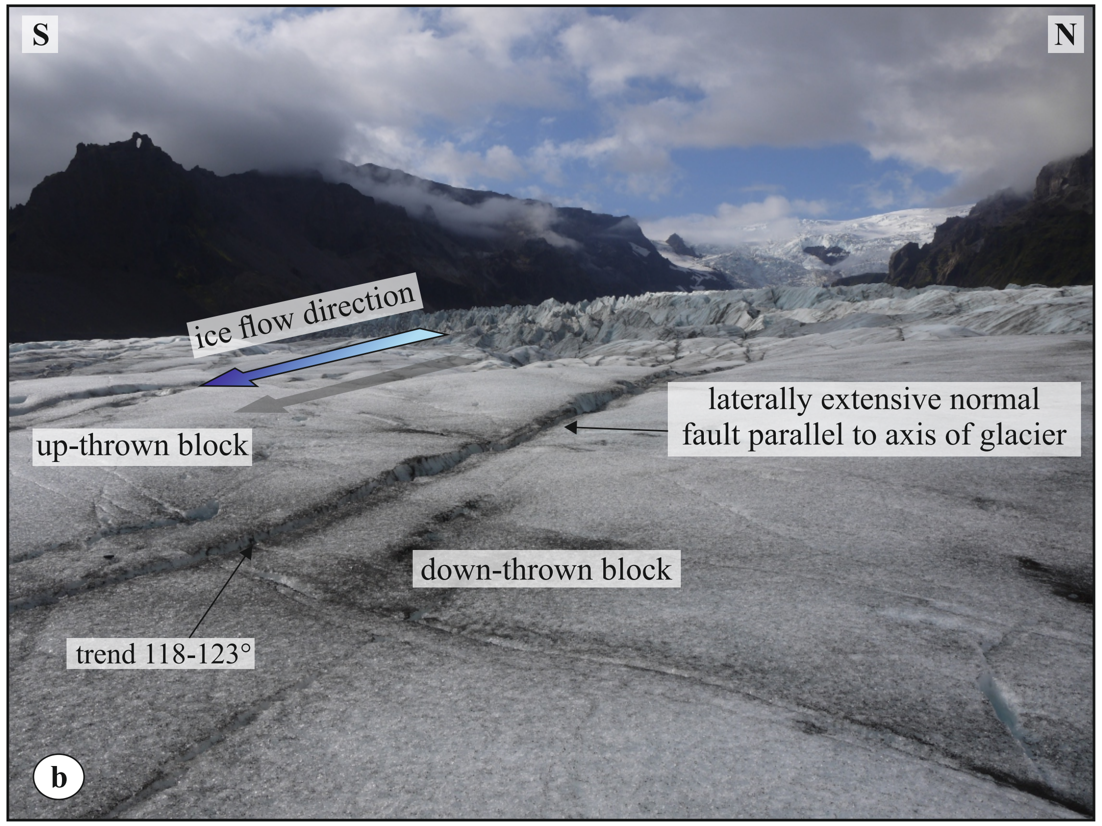

Location: Northing 384809 Easting 623610

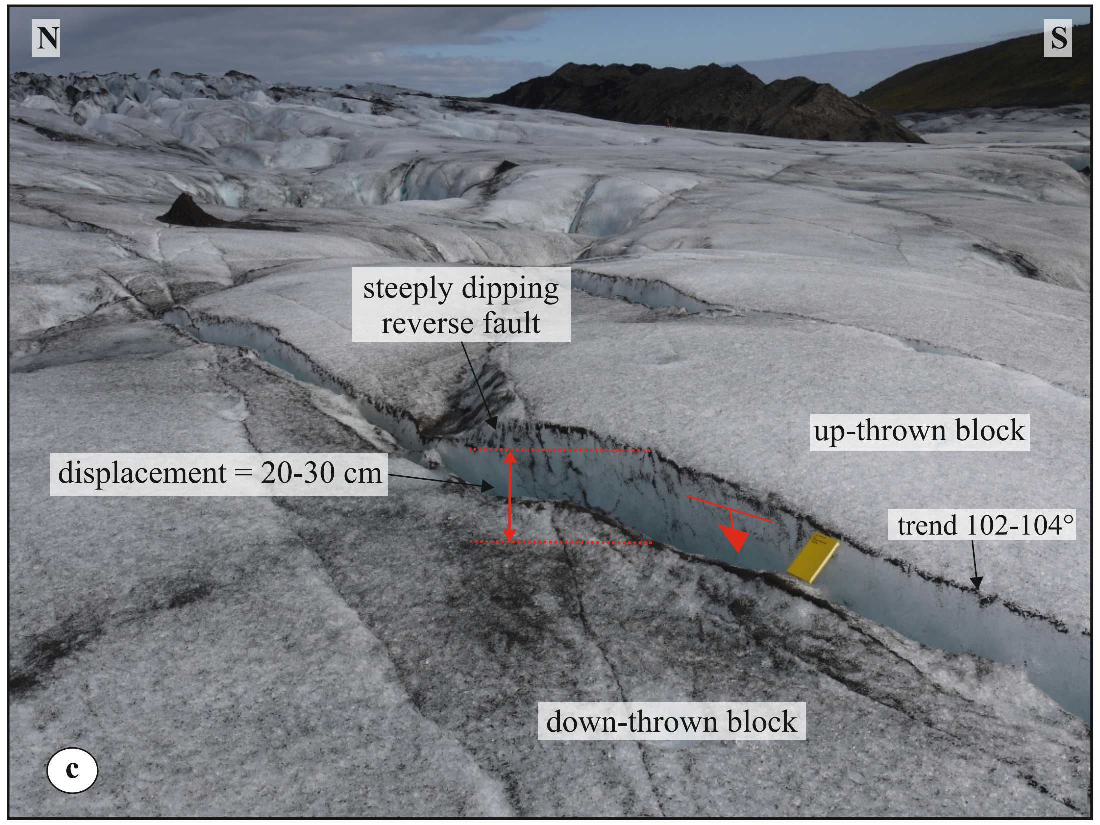

Location: Northing 384742 Easting 623727

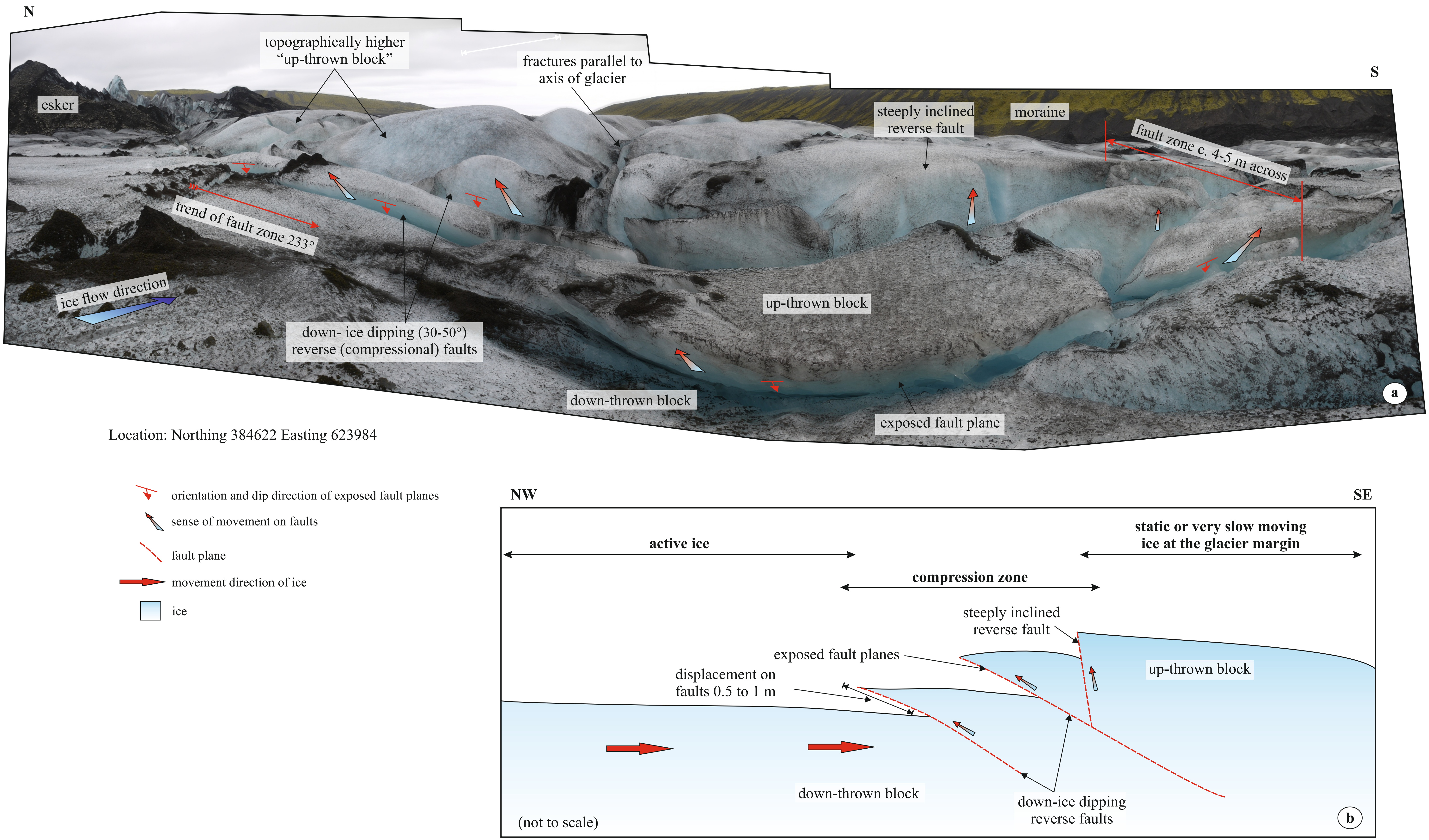
N
S
esker
topographically higher
“up-thrown block”
fractures parallel to
axis of glacier
steeply inclined
reverse fault
moraine
fault zone c. 4-5 m across
trend of fault zone 233°
ice flow direction
up-thrown block
down- ice dipping (30-50°)
reverse (compressional) faults
down-thrown block
exposed fault plane
a
Location: Northing 384622 Easting 623984
orientation and dip direction of exposed fault planes
sense of movement on faults
fault plane
movement direction of ice
ice
NW
SE
active ice
static or very slow moving
ice at the glacier margin
compression zone
steeply inclined
reverse fault
exposed fault planes
displacement on
faults 0.5 to 1 m
up-thrown block
down-thrown block
down-ice dipping
reverse faults
(not to scale)
b

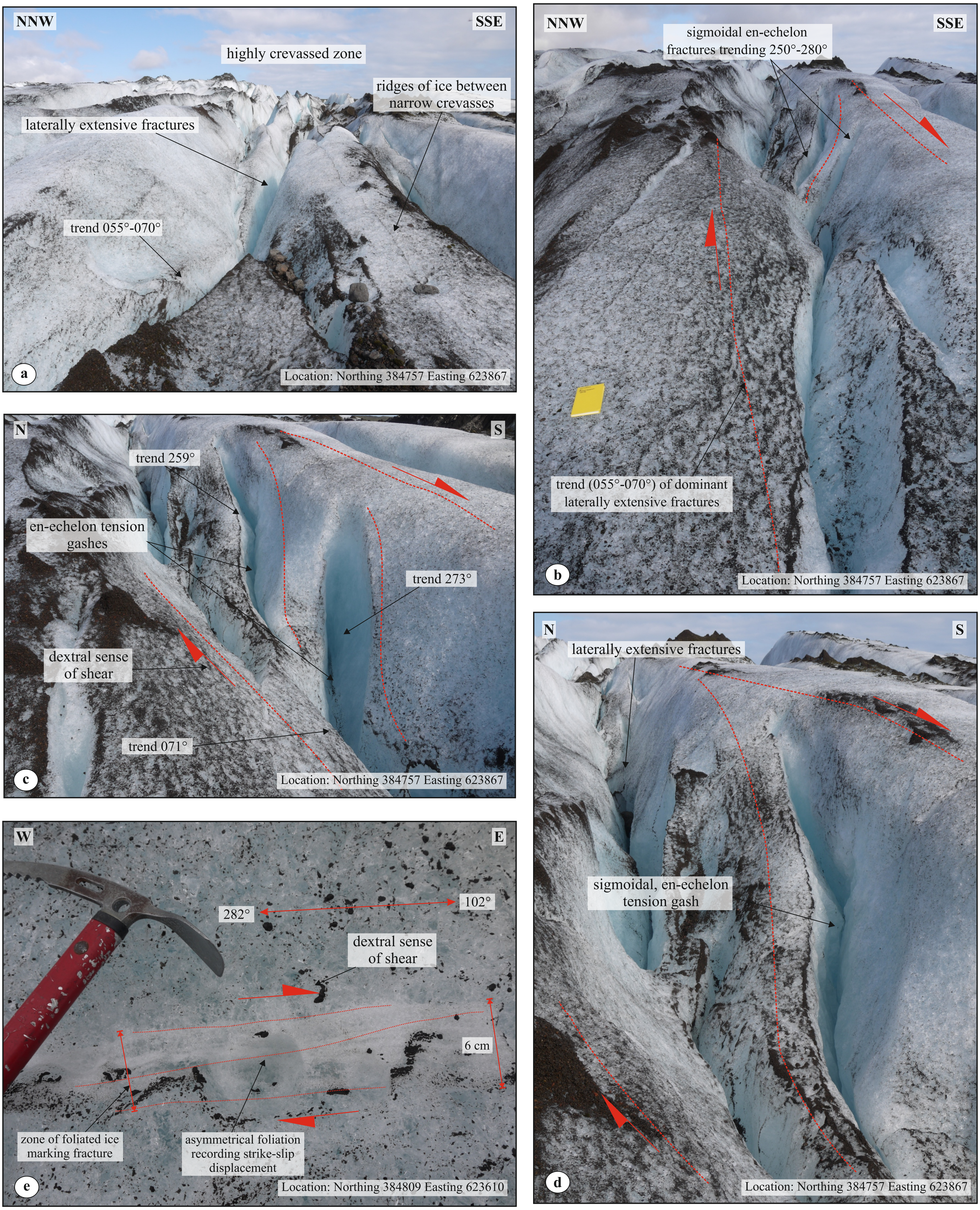
NNW
SSE
highly crevassed zone
ridges of ice between narrow crevasses
laterally extensive fractures
trend 055°-070°
a
Location: Northing 384757 Easting 623867
NNW
SSE
sigmoidal en-echelon fractures trending 250°-280°
trend (055°-070°) of dominant laterally extensive fractures
b
Location: Northing 384757 Easting 623867
N
S
trend 259°
en-echelon tension gashes
trend 273°
dextral sense of shear
trend 071°
c
Location: Northing 384757 Easting 623867
N
S
laterally extensive fractures
sigmoidal, en-echelon tension gash
d
Location: Northing 384757 Easting 623867
W
E
282°
102°
dextral sense of shear
6 cm
zone of foliated ice marking fracture
asymmetrical foliation recording strike-slip displacement
e
Location: Northing 384809 Easting 623610

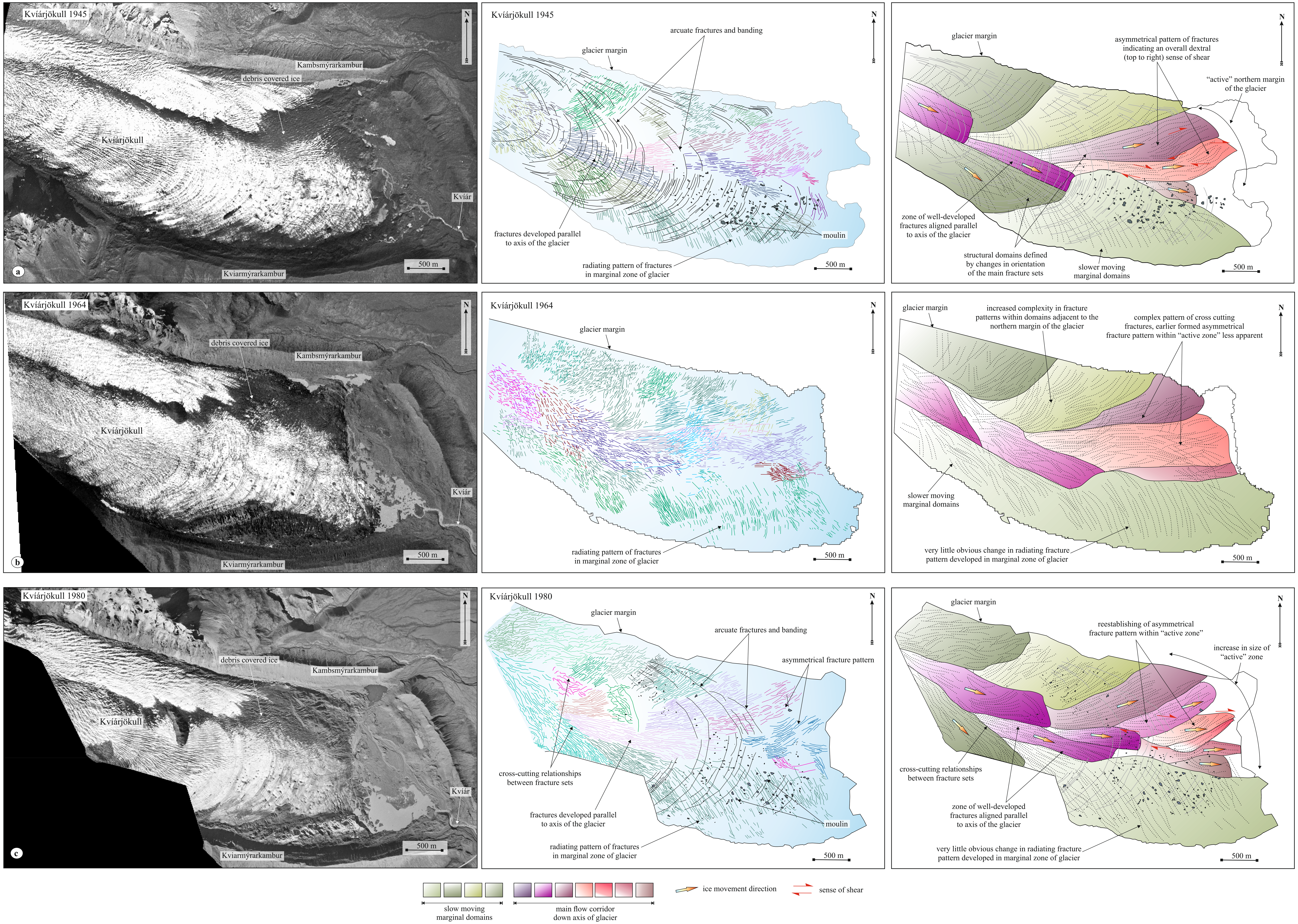

Kviárjökull 1945
N
Kambsmýrarkambur
debris covered ice
Kviárjökull
Kviár
500 m
Kviarmýrarkambur
a
Kviárjökull 1945
arcuate fractures and banding
glacier margin
fractures developed parallel
to axis of the glacier
radiating pattern of fractures
in marginal zone of glacier
moulin
glacier margin
asymmetrical pattern of fractures
indicating an overall dextral
(top to right) sense of shear
"active" northern margin
of the glacier
zone of well-developed
fractures aligned parallel
to axis of the glacier
structural domains defined
by changes in orientation
of the main fracture sets
slower moving
marginal domains
Kviárjökull 1964
debris covered ice
Kambsmýrarkambur
Kviárjökull
Kviár
Kviarmýrarkambur
b
Kviárjökull 1964
glacier margin
radiating pattern of fractures
in marginal zone of glacier
glacier margin
increased complexity in fracture
patterns within domains adjacent to the
northern margin of the glacier
complex pattern of cross cutting
fractures, earlier formed asymmetrical
fracture pattern within "active zone" less apparent
slower moving
marginal domains
very little obvious change in radiating fracture
pattern developed in marginal zone of glacier
Kviárjökull 1980
debris covered ice
Kambsmýrarkambur
Kviárjökull
Kviár
Kviarmýrarkambur
c
Kviárjökull 1980
glacier margin
arcuate fractures and banding
asymmetrical fracture pattern
cross-cutting relationships
between fracture sets
fractures developed parallel
to axis of the glacier
radiating pattern of fractures
in marginal zone of glacier
moulin
glacier margin
reestablishing of asymmetrical
fracture pattern within "active zone"
increase in size of
"active" zone
cross-cutting relationships
between fracture sets
zone of well-developed
fractures aligned parallel
to axis of the glacier
very little obvious change in radiating fracture
pattern developed in marginal zone of glacier
slow moving
marginal domains
main flow corridor
down axis of glacier
ice movement direction
sense of shear

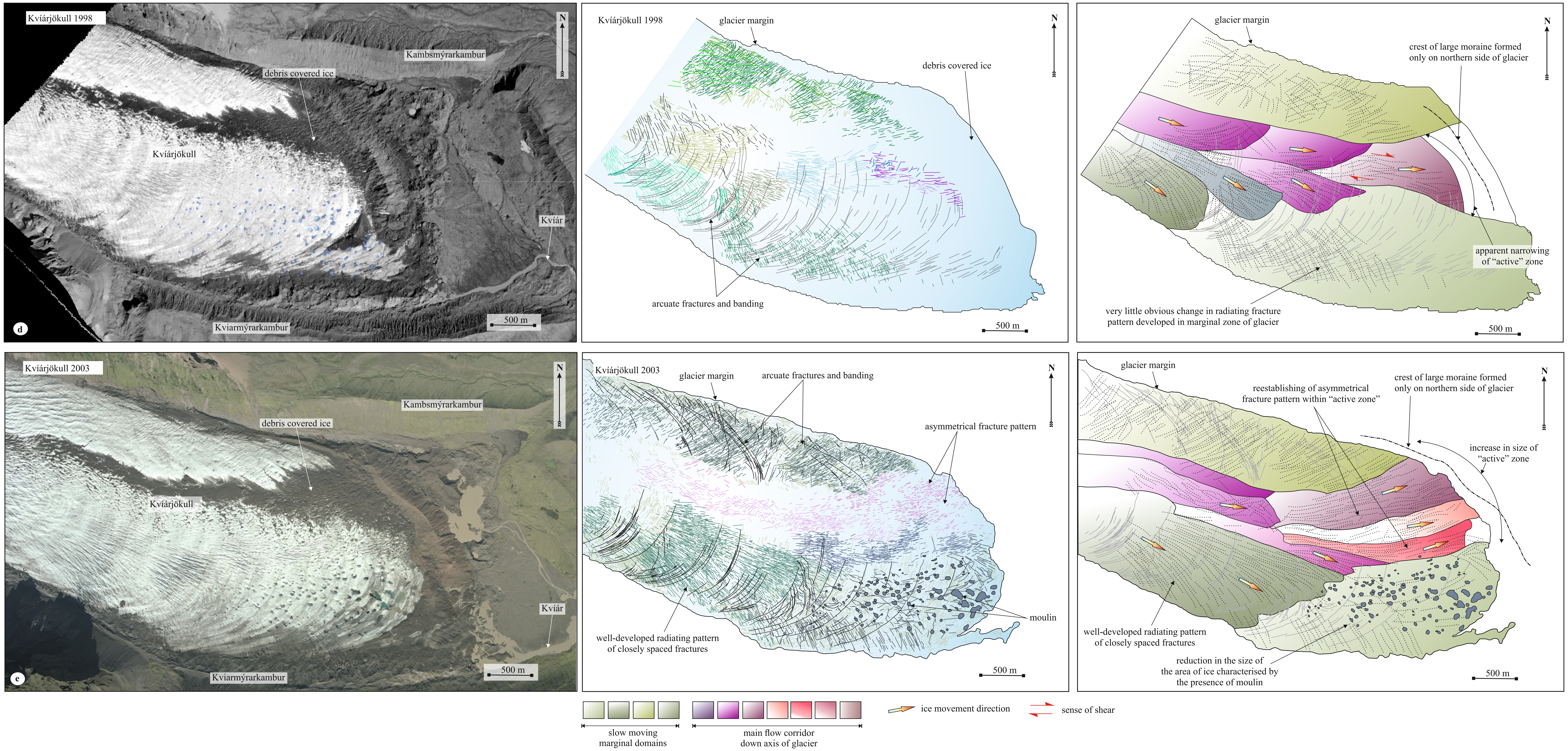

Kviárjökull 1998
N
Kambsmýrarkambur
debris covered ice
Kviárjökull
Kviár
500 m
Kviarmýrarkambur
d
Kviárjökull 1998
glacier margin
debris covered ice
arcuate fractures and banding
500 m
glacier margin
crest of large moraine formed only on northern side of glacier
apparent narrowing of "active" zone
very little obvious change in radiating fracture pattern developed in marginal zone of glacier
500 m
Kviárjökull 2003
Kambsmýrarkambur
debris covered ice
Kviárjökull
Kviár
500 m
Kviarmýrarkambur
e
Kviárjökull 2003
glacier margin
arcuate fractures and banding
asymmetrical fracture pattern
moulin
well-developed radiating pattern of closely spaced fractures
500 m
glacier margin
reestablishing of asymmetrical fracture pattern within "active zone"
crest of large moraine formed only on northern side of glacier
increase in size of "active" zone
well-developed radiating pattern of closely spaced fractures
reduction in the size of the area of ice characterised by the presence of moulin
500 m
slow moving marginal domains
main flow corridor down axis of glacier
ice movement direction
sense of shear